April 2020

The Effects of Skeletal Muscle Specific Cpt1b Knock Out on Genetically Obese Ay Mice

Allison Stone

THE EFFECTS OF SKELETAL MUSCLE SPECIFIC CP1B KNOCK OUT ON GENETICALLY OBESE A^Y MICE

A Thesis

Submitted to the Graduate Faculty of the
Louisiana State University and
Agricultural and Mechanical College
in partial fulfillment of the
requirements for the degree of
Master of Science

in

The Department of Nutrition and Food Sciences

by
Allison C. Stone
B.S., Southeastern Louisiana University, 2017
May 2020

Table of Contents

List of Tables

List of Figures

Abbreviations

Acaca…… Acetyl-CoA Carboxylase Alpha

Acox1……. Acyl-CoA Oxidase 1

Bcat2…… Branched Chain Anino Acid Transaminase

Bckdha……. Branched Chain Keto Acid Dehydrogenase

Cpt1a……... Carnitine Palmitoyl Transferase Alpha

Cs…… Citrate Synthase

Ech1……... Enoyl-CoA Hydratase

Fabp3……. Fatty Acid Binding Protein 3

Fasn……... Fatty Acid Synthase

Fatp1…… Fatty Acid Transport Protein 1

Fgf21……... Fibroblast Growth Factor 21

Gdf15……... Growth Differentiation Factor 15

Hadha…… Hydroxyacyl-CoA Dehydrogenase

Pck1…… Phosphoenolpyruvate Carboxykinase 1

Pdha1…… Pyruvate Dehydrogenase

Plin5……. Perilipin 5

Scd1…… Steroyl-CoA Desaturase

Abstract

Fatty acid oxidation inhibition is one approach to reducing blood glucose levels in type II diabetes. Skeletal muscle specific Carnitine Palmitoyltransferase 1b knockout mice ($Cpt1b^{m-/-}$) cannot transport long-chain fatty acids into the mitochondria to be oxidized in order to produce energy. $Cpt1b^{m-/-}$ mice have debilitated fat oxidation, less fat mass and improved glucose utilization compared to control C57BL/6 mice fed a 25% fat diet.

We hypothesized that *CPT1b* inhibition could reduce fat mass and lower blood glucose levels in a genetic mouse model of obesity and diabetes. To test this, we bred $Cpt1b^{m-/-}$ mice to A^Y mice. A^Y mice, also referred to as lethal yellow mice, are mutated at the mouse *agouti* locus causing a yellow coat. A^Y mice are prone to obesity, diabetes, tumors and cancers. The goal of this study was to determine the effect of extended inhibition of fatty acid transport into skeletal muscle mitochondria in A^Y: $Cpt1b^{m-/-}$ mice.

Compared to A^Y mice, A^Y: $Cpt1b^{m-/-}$ mice were more insulin sensitive and glucose tolerant. A^Y: $Cpt1b^{m-/-}$ mice showed improved performance on glucose and insulin tolerance tests despite minimal differences in fat mass between groups. However, liver weights of A^Y: $Cpt1b^{m-/-}$ mice were significantly less than liver weights of A^Y mice.

Introduction

1.1. Modern Treatment Plans for Obesity and Type 2 Diabetes

Current treatment plans for obesity and type 2 diabetes include lifestyle-intervention programs or administration of metformin. Both treatments have been shown to reduce the incidence of diabetes in high risk individuals (Knowler, 2002). Thiazolidinediones (TZDs) drugs serve as insulin sensitizers through decreasing the production and increasing the disposal of glucose. TZD has been shown to activate AMPK and increase mitochondrial biogenesis in adipose tissue (Wilson-Fritch et al., 2004). Mitochondrial inhibition in skeletal muscle also improves insulin sensitivity (Pagel-Langenickel, Bao, Pang, & Sack, 2010). Investigation of diabetic and obesogenic mouse models aids in the development of new treatment plans for the prevention and amelioration of obesity and type 2 diabetes.

1.2. History of A^Y Mice

Lethal yellow (A^Y) mutated mice are a genetically obese and diabetic mouse model commonly used for the study of obesity and insulin resistance. A^Y mice have a mutation on chromosome 2 at the *agouti* locus. All surviving mice with the A^Y mutation are heterozygous for the A^Y mutation. Mice that are homozygous for the A^Y mutation will result in embryonic lethality before implantation (Iwatsuka, Shino, & Suzuoki, 1970). This mutation causes these mice to overexpress agouti which results in a completely yellow coat color and a genetically obese and diabetic mouse model. A^Y mice are prone to yellow obese syndrome which consists of obesity, hyperglycemia, hyperinsulinemia, increased tumor incidence and increased skeletal and muscle growth (Miltenberger, Mynatt, Wilkinson, & Woychik, 1997). It is common for A^Y mice to become infertile a few months after birth (Iwatsuka et al., 1970). In a preferential macronutrient study, A^Y mice consumed higher amounts of fat than carbohydrate and protein. This preference for fat could explain their increase in overall body fat content. Antagonists to the melanocortin receptors (MC-Rs) or increased palatability could be credited for the preferential consumption of fat in these mice. Liver weights for A^Y mice, expressed as absolute weight or as percent of body weight, were both found to be significantly heavier relative to control mice. (Koegler, Schafffhauser, Mynatt, York, & Bary, 1999)

The *agouti* gene locus manages the distribution of eumelanin (brown and black) and pheomelanin (red and yellow) for coat pigmentation. Agouti is a small protein made up of 131 amino acids (Wang & Majzoub, 2011). Agouti antagonizes α-melanocyte-stimulating hormone (α-MSH) by blocking the actions of follicular melanocytes at the melanocortin 1 receptor (MC1R). MC1R is a highly expressed G protein-coupled receptor found in melanocytes. Melanocytes are cells responsible for pigment production. Under normal circumstances, α-MSH would activate MC1R which would elevate cAMP levels and increase the production of eumelanin. If agouti is present, it serves as an antagonist to MC1R which results in decreased eumelanin and increased pheomelanin production (Nachman, Hoekstra, & D'Agostino, 2003). This is what causes the phenotypic yellow coat color observed in heterozygous A^Y mice. Agouti can also serve as an antagonist to neural melanocortin receptors, MC4R and MC3R; however, the interaction with MC3R is notably weaker (Wang & Majzoub, 2011). The melanocortin system only has two known antagonists, agouti related protein (AGRP) and agouti (Tao, 2010).

The paracrine signaling molecule known as agouti related protein (AGRP) is known to regulate body weight. It serves as an antagonist to both neural melanocortin receptors, MC3R and MC4R (Ollmann, 1998). It is expressed at highest amounts in the hypothalamus and adrenal medulla. Lower levels of expression can be seen in the testis, lung and kidney (Wang & Majzoub, 2011). Normally, leptin is released from adipose tissue and it acts upon melanocortin neurons or AGRP neurons. This results in increased α-MSH and decreased AGRP. When α-MSH binds MC4R, it inhibits food intake and increases energy expenditure. If AGRP blocks α-MSH, food intake is increased and energy expenditure decreases (Dutia et al., 2013). At the melanocortin receptor in the skin, MC1R, agouti blocks α-MSH from binding which results in a yellow coat color. Since agouti can also antagonize MC4R and MC3R, it also has the ability to block neural α-MSH. Therefore, a ubiquitous promoter driving the overexpression of agouti results in a yellow coat color when the α-MSH in the skin is blocked by agouti as well as obesity when the α-MSH in the brain is blocked by agouti. The phenotype associated with the heterozygous lethal yellow (A^y) mutated mice can be explained by the overexpression of agouti; however, the embryonic lethality found in mice that are homozygous for this mutation is caused by the deletion of another gene.

The A^Y mutation is brought about by a 170 kb excision which removes a gene known as *Raly* which is positioned upstream of the *agouti* locus. The *Raly* gene promoter and first noncoding exon is all that remains after the deletion (Michaud et al., 1994). Essentially, what happens is *Raly's* promoter splices into the open reading frame of the agouti gene and begins to drive the expression of agouti which results in ubiquitous overexpression of agouti. The excision of the *Raly* gene is believed to be the cause of lethality in mice that are homozygous for this mutation (Michaud et al., 1994). The genetically induced obesity and insulin resistance found in these mice makes for a desirable model for obesogenic and diabetic research.

1.3. The Skeletal Muscle Specific Cpt1b$^{m-/-}$ Knock Out Mice

The enzyme *Cpt1* resides in the outer mitochondrial membrane and is responsible for catalyzing the reaction necessary for the transport of long chain fatty acids into the inner mitochondrial membrane where beta oxidation can occur. The *Cpt1* isoform of interest is *Cpt1b* since this is the form found in skeletal muscle. *Cpt1b* is one of three isoforms with the other two being *Cpt1a* and *Cpt1c*. *Cpt1a* is expressed ubiquitously with exceptions being skeletal muscle and brown adipose tissue. Its largest expression is found in the liver. *Cpt1b* is expressed in heart, skeletal muscle and brown adipose tissue and *Cpt1c* can be found in the brain and testes (Rufer, Thoma, & Hennig, 2009). When *Cpt1b* is knocked out in skeletal muscle, long chain fatty acyl-CoAs cannot be conjugated to L-carnitine. Since acyl-CoA cannot cross into the mitochondrial matrix through simple diffusion, fatty acid beta oxidation is inhibited in skeletal muscle (Cobb & Dukes, 1998).

Through the use of transgenes and mouse genome manipulation, knock out mouse models are designed to allow for a deeper understanding of diabetes and obesity. The *Cpt1b* muscle specific knock out in this study was achieved by crossing mice with floxed alleles of *Cpt1b* to Mlc1f-Cre transgenic mice for skeletal muscle specific deletion of *Cpt1b*, but not cardiac tissue (Shawna E. Wicks et al., 2015). Previous studies using this mouse model noted that despite ectopic lipid accumulation in muscle, Cpt1b$^{-/-}$ mice maintained insulin sensitivity while on a moderate fat (25% kcal) breeder chow diet (S. E. Wicks et al., 2015). Additionally, skeletal muscle specific Cptlb$^{m-/-}$ mice had improved glucose uptake along with induced *Fgf21*

expression in muscle. A double knockout mouse model of *Cpt1b* and *Fgf21* showed a partial negation in improved glucose utilization in comparison to *Cpt1b* knock outs. *Fgf21* appeared to be partially responsible for the increase in glucose utilization in a manner that was independent of the stress signaling pathway but dependent on AMPK and Akt1 signaling (Vandanmagsar et al., 2016).

1.4. Controversial Research Regarding Inhibition and Upregulation of B-Oxidation in Skeletal Muscle

Whether overexpression or inhibition of *Cpt1* in skeletal muscle is needed to improve insulin resistance is a controversial topic with literature supporting both concepts. *Cpt1* overexpression in skeletal muscle was found to be sufficient for mitigating lipid-induced insulin resistance in a rat study. Overexpression was achieved through *in vivo* electro transfer of a purified *Cpt1* plasmid via direct injection into the tibialis anterior of rats. Extensor digitorum longus (EDL) was the muscle used for measuring glucose uptake due to its close proximity with the tibialis anterior. Overexpression of *Cpt1* in the EDL of rats fed high fat diet for a 4-week period enhanced insulin stimulated glucose uptake to similar levels seen in the control rats fed a chow diet (Bruce et al., 2009). Similar results were found in a study where increased B-oxidation in muscle cells was enough to increase glucose metabolism stimulated by insulin and protect against fatty acid induced insulin resistance. B-oxidation in myocytes was enhanced by transducing myotubules with an adenovirus encoding *Cpt1*. They proposed that enhanced B-oxidation in muscle was enough to exert an insulin sensitizing effect despite no change in intramyocellular lipid accumulation (Perdomo et al., 2004). A study using myotubules found overexpression of *Cpt1* protected against fatty acid induced insulin resistance. This overexpression lead to a reduction in the accumulation of lipid in muscle tissue thus diminishing the likelihood of fulfilling the lipotoxic model of skeletal muscle insulin resistance hypothesis (Sebastian, Herrero, Serra, Asins, & Hegardt, 2007).

Contrary to the findings above, another study found deficiency in *Cpt1b* protected mice from diet induced obesity. The animals in this study had a global heterozygous $Cpt1b^{+/-}$ knockout and therefore showed that partial inhibition of *Cpt1b* was sufficient to protect from insulin resistance when fed a high fat diet for up to 5 months (Kim, He, et al., 2014). A later study found the partial knock out mice developed severe insulin resistance after 7 months on the high fat diet, providing further justification for our homozygous knock out model (Kim, Moore, et al., 2014). Oxfenicine, a *Cpt1* inhibitor, was used to hinder *Cpt1* activity consequently alleviating insulin resistance associated with diet induced obesity. Findings included increased carbohydrate utilization and improvement in insulin signaling in skeletal muscle, proposing a possible Randle Cycle in skeletal muscle (Keung et al., 2013). Malonyl-CoA decarboxylase ($mcd^{-/-}$) knockout mice were generated to inhibit fat catabolism in skeletal muscle. Malonyl-CoA decarboxylase (MCD) is the enzyme that converts malonyl CoA to acetyl CoA and CO_2. In doing so, MCD prevents the buildup of malonyl CoA, a known inhibitor of *Cpt1*. Therefore, when MCD is knocked out, malonyl CoA will build up and inhibit *Cpt1* and thus fatty acid oxidation in skeletal muscle. Results from this study showed $mcd^{-/-}$ mice resisted diet induced glucose intolerance despite having higher than normal intramuscular levels of long-chain acyl-CoAs (Koves et al., 2008).

1.5. Existing Theories for Skeletal Muscle Insulin Resistance

This leads to discussion of two competing theories pertaining to skeletal muscle insulin resistance. The first theory states that excess ectopic lipid buildup leads to insulin resistance because lipid overload interferes with insulin signaling. Hardy et al. says the accumulation of ectopic lipid in skeletal muscle may cause insulin resistance through the formation of toxic intermediates; for example, saturated fats have presented evidence of increased ceramide production, which seems to augment insulin resistance (Hardy, Czech, & Corvera, 2012). A buildup of diacylglycerols (DAGs) has been shown to activate isoforms of novel protein kinase C which leads to phosphorylation of insulin receptor substrate-1 (IRS-1), resulting in impaired downstream insulin signaling. The term "lipotoxicity" has been coined to define the state in which excess lipid accumulation leads to insulin resistance in skeletal muscle (Badin et al., 2011).

The contending theory states that excess ectopic lipids are partially broken down by mitochondria, and the incompletely broken-down intermediates are toxic, which then interfere with insulin signaling. A study found skeletal muscle insulin resistance to be indicative of elevated fatty acid catabolism rates which resulted in incomplete fatty acid B-oxidation and a large portion of fatty acids entering the mitochondria resulting in only partial degradation. Further characteristics of skeletal muscle insulin resistance from this study included debilitated switching of fuel substrates between the fed-to-fasted transition ("metabolic inflexibility") and a deficiency in multiple Krebs cycle intermediates (Koves et al., 2008). Additionally, inhibition of fatty acid transport into the mitochondria of skeletal muscle resulted in a rather remarkable phenotype where mice remained insulin sensitive despite ectopic lipid accumulation in the muscle (S. E. Wicks et al., 2015).

Since *Cpt1b* skeletal muscle specific knockout mouse models have been shown to have ectopic lipids yet no insulin resistance, we favor the latter theory. Without *Cpt1b* the mitochondria are not capable of breaking down fatty acids; therefore, the culprit for insulin sensitivity interference may be the toxic incompletely broken-down intermediates rather than ectopic lipid buildup.

Based off the data mentioned above regarding *Cpt1* overexpression and insulin sensitivity, increased capacity for breaking down lipids may also prevent the buildup of toxic intermediates. However, some warn against the use of pharmacologic strategies geared toward boosting B-oxidation to alleviate muscle insulin resistance, suggesting fatty acids must penetrate muscle mitochondria in order to exert insulin-desensitizing effects. Their evidence proposes obesity-associated glucose intolerance arising from metabolic overload of muscle mitochondria which could potentially result from excessive B-oxidation (Koves et al., 2008). Another study found similar results against the use of excessive B-oxidation for ameliorating skeletal muscle insulin resistance. While studying gain-and-loss-of-function of peroxisome proliferator-activated receptor-α (PPAR-α) in regards to the development of insulin resistance, transgenic mice overexpressing PPAR-α in muscle resulted in increased rates of fatty acid oxidation along with glucose intolerance. PPAR-α null mice were protected from insulin resistance. Oxfenicine, an inhibitor of skeletal muscle *Cpt1*, was administered to the transgenic mice overexpressing PPAR-α, resulting in lipid accumulation in skeletal myocytes and improved glucose tolerance (Finck et al., 2005). Herein, we align with the hypothesis for protection from skeletal muscle insulin resistance with reduced rather than excessive fatty acid oxidation.

1.6. Combinational Approach in this Study

The overall objective of this project is to determine if inhibiting skeletal muscle mitochondrial fatty acid oxidation can help improve insulin resistance and weight loss in a genetically obese and diabetic mouse model. The hypothesis made states that carnitine palmitoyl transferase (*Cpt1b*) inhibition specifically in skeletal muscle could improve fat mass and blood glucose levels in a genetic mouse model of obesity and diabetes. In an attempt to further understand how inhibiting fatty acid oxidation mediates insulin resistance and obesity, carnitine palmitoyltransferase (*Cpt1b*) was knocked out in skeletal muscle of a genetically obese mouse model known as lethal yellow (A^Y) mutated mice. Four genotypes were included: Control mice, $Cpt1b^{m-/-}$ mice, A^Y mice and A^Y: $Cpt1b^{m-/-}$ mice with focus throughout being primarily on A^Y: $Cpt1b^{m-/-}$ mice since the $Cpt1b^{m-/-}$ phenotype has been well established in prior studies (S. E. Wicks et al., 2015) (Vandanmagsar et al., 2016; Warfel et al., 2016). All mice from this study came from the C57BL/6 background.

Methods

2.1. Animal Studies

Animal studies took place at Pennington Biomedical Research Center's American Association for the Accreditation of Laboratory Animal Care-approved facility, with mice receiving a standard chow diet, comprised of 25% fat, 55% carbohydrate and 20% protein (Mouse Chow Diet no. 5015; LabDiet). All procedures were in agreeance with the NIH Guide for the Care and Use of Laboratory Animals and authorized by the Institutional Animal Care and Use Committee. The majority of the mice used in this experiment were between the ages of 4 to 8 months of age unless stated differently.

2.2. Animal Procedures

Body composition (fluid, fat mass, lean mass) was measured using a Bruker NMR Minispec (Bruker Corporation). Mice were weighed on a scale prior to each use of Minispec and bodyweights were recorded in grams. Serum and plasma collections were performed by submandibular bleed. Following a 4 hour fast, glucose tolerance tests (GTTs) were performed by intraperitoneal injection of 10% D-glucose (40 mg of glucose per mouse). Blood glucose was measured with a glucometer at 0, 20, 40 and 60 minutes via tail end snip. Insulin Tolerance tests (ITTs) were performed while in the fed state, using an intraperitoneal dose of 0.04 units (U) per mouse. Measurements were taken with a glucometer at 0, 20, 40 and 60 minutes via tail end snip.

2.3. Metabolic Profiling

ELISA kits were used for measurement of 4 hour fasted serum insulin (Ultra-Sensitive Mouse Insulin ELISA kit; Crystal Chem, Inc. #90080) and Triglycerides (TAGs) (Triglyceride-H; Wako Diagnostics) and fed serum FGF21 (BioVendors). Liver TAGs were also measured (Triglyceride-H; Wako Diagnostics). Glycogen was measured in liver using a commercial kit (65620; Abcam) with instructions provided by the manufacturer.

2.4. Hepatic Fluid Measurement

Tissues were collected and patted free of exogenous blood prior to being snap frozen in liquid nitrogen. This procedure was precisely replicated for all livers collected. Aliquots ranging from 20-100 mg were collected from each whole liver for this dehydration experiments. Each aliquot was weighed before being placed in the NAPCO vacuum oven (model 5831). Samples were left in the vacuum overnight with the temperature control set at a 2.5 and vacuum at ≈ 5 Hg. Desiccated samples were reweighed the next morning. The difference between the wet weight and desiccated weight was recorded for each sample and perceived as fluid level. Next, grams of fluid per grams of wet weight were determined by dividing the difference (fluid amount) for each sample by the weight of the aliquot prior to dehydration for each sample. Total fluid was determined by multiplying the value for grams of fluid per grams of wet weight for each sample with the original whole liver weight recorded at necropsy for each sample.

2.5. qRT-PCR

Total RNA from mouse tissue (snap frozen on liquid nitrogen at the collection) was isolated using a RNeasy Mini Kit (Qiagen) and DNase was used to degrade DNA. cDNA synthesized with the iScript cDNA synthesis kit was used for qRT-PCR with the SYBR Green system (Bio-Rad). qRT-PCR was conducted using DDCT assay. Mouse cyclophilin B was used as the housekeeping-gene control for normalization of gene expression. Previously our lab demonstrated that all target and control genes showed appropriate amplification using standard curves. Primer details are provided in table 1.

2.6. Histology

Liver from mice were harvested and fixed with formalin. Then the tissues were embedded in paraffin and sectioned and stained with H&E at the Cell Biology and Bioimaging Core Facility at Pennington Biomedical Research Center. Images were viewed at a magnification of 5x using NDP.view2 software.

2.7. Generation of Skeletal Muscle-Specific Cpt1b KO Mice

Knock out mice were achieved through the use of the cre-lox system. This technology requires the generation of a cre-lox mouse via breeding. Typically, this is produced by mating a mouse positive for cre with a mouse with lox P sights flanking the gene of interest. Cre serves as a recombinase which is guided by a specific promoter which in this case is Mlc1f (Laboratory, 2006). The Mlc1f-Cre transgene is used to ablate Cpt1b specifically in skeletal muscle but it remains highly expressed in cardiac tissue. This is because the Mlc1f promoter is specific for skeletal muscle. Mlc1f is one of two independent promoters located at the myosin light chain locus. These promoters are differentially activated during skeletal muscle development. The second promoter is known as Mlc3f. The Mlc1f promoter is used for skeletal muscle specific knock downs because the Mlc3f promoter has low level expression in the left atria and ventricle of mouse cardiac tissue (Kelly, Alonso, Tajbakhsh, Cossu, & Buckingham, 1995). When the cre recombinase mouse is bred with the flanked lox P gene of interest mouse, cre will cut half of each lox P site resulting in the excision of the gene of interest from the genome and recombination of the remaining lox P halves. For this experiment, cre positive mice were bred to floxed Cpt1b mice in order to achieve a skeletal muscle specific Cpt1b knock out. Cpt1b muscle specific knock out mice were achieved by breeding Mlc1f-Cre recombinase mice (from Gerald Bothe, Wadsworth Center, Albany, NY) that were backcrossed for 10 generations to C57BL6 mice; therefore, all mice are from the C57BL6 background. All chimeric mouse production and gene targeting was executed by the Transgenic Core at Pennington Biomedical Research Center.

Table 1. Primers and Sequences. This is a comprehensive list of forward and reverse primers used in this study.

Gene Symbol	Reference Sequencing ID	Forward Primer	Reverse Primer
Hadha	NM_178878	TGACGCTGGTTATCTTGCTG	ATCAGGGCCTTCGATTCTTT
Ech1	NM_016772	TCGCTACTGCACTCAGGATG	AGCAGCCAAGCCCATATCTA
Bckdha	NM_007533	GTGGGATGAGGAACAGGAGA	CTTGGGTTCGGCTTTAGCTT
Bcat2	NM_001243052	CGCTTCCAGAAGGAACTGAA	CACACCCGAAACATCCAATC
Cd36	NM_001159555	GCAAAGAACAGCAGCAAAATC	TCCTCGGGGTCCTGAGTTAT
Fatp1	NM_011977	GGTGGTACTGCGCAAGAAGT	AGCGGCAGATTTCACCTATG
Fabp3	NM_010174	GACGAGGTGACAGCAGATGA	CTGCACATGGATGAGTTTGC
Plin5	NM_001077348	CTTCCTGCCCATGACTGAG	ACCCCAGACGCACAAAGTAG
Acox1	NM_015729	CTTCGAGGGGGAGAACACT	CCCGACTGAACCTGGTCATA
Fgf21	NM_020013	TTCTTTGCCAACAGCCAGAT	GTCCTCCAGCAGCAGTTCTC
Cs	NM_026444	CGGGAGGGCAGCAGTATCGG	ACCACCCTCATGGTCACTATGGATG
Cyclophilin	NM_011149	TCCATCGTGTCATCAAGGACTT	CTCATCTGGGAAGCGCTCA
Pdha1	NM_008810	GGTTGCTTCCCGTAATTTTG	GTGAGCACTGTGGTGACTGG
Gdf15	NM_ 23886	GCTGTCCGGATACTCAGTCC	GTAGGCTTCGGGGAGACC
Acaca	NM_ 107476	ATGGTTGAGTGGGTTTTTTGACTAT	CCTAACCTGGCTCTGCCAACT
Fasn	NM_ 14104	GATCCTGGAACGAGAACACGAT	TCGTGTCAGTAGCCGAGTCA
Scd1	NM_ 20249	CCGGGAGAATATCCTGGTTT	TAGTCGAAGGGGAAGGTGTG
Cpt1a	NM_ 12894	CATGATTGCAAAGATCAATCGG	CTTGACATGCGGCCAGTG
Pck1	NM_ 18534	GGTGTCCCCCTTGTCTATGAAG	ATCTTGCCCTTGTGTTCTGCA

2.8. Generation of Skeletal Muscle-Specific Cpt1b KO and A^Y Mutated Mice

The A^Y:Cpt1b$^{m-/-}$ mice are double mutated and may be referred to as Double Mutants (DMut Mice). The Cpt1b knock out mice were generated as described above. The Cpt1b knock out mice were then crossed with A^Y mice (Jackson Laboratory) in order to achieve the double mutated mice.

2.9. Confirmation of Genotype

Mouse DNA is obtained from tail end snips or ear punches. Snips are digested using a tail lysis buffer. Following digestion, DNA is isolated through a series of separations with columns using centrifugation. DNA is amplified via polymerase chain reaction (PCR), then run on an agarose gel. Upon completion of electrophoresis, the gel is imaged using the Image Lab 4.0.1 Software.

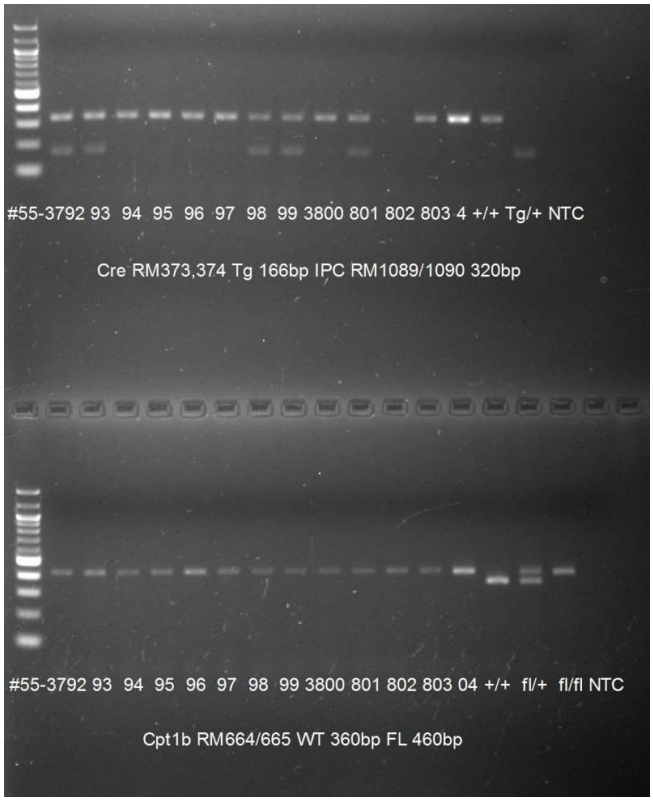

Figure 1. Genotyping for Cre and Cpt1b. This gel image demonstrates how mice are genotyped for cre recombinase and floxed Cpt1b.

Knock out mice are confirmed by checking for cre recombinase and lox P sites. When checking for cre, an internal processing control (IPC) is used in order to reduce the chances of false negatives. Therefore, all mice should show a band at 320bp which is indicative of the IPC. The IPC amplicon is added to the extracted DNA for each sample before the DNA is added to the well of the gel. For detection of the cre gene, forward and reverse primers for the cre gene are

used to produce amplicons with the size of 166 bp. Therefore, cre positive mice will show an additional band at 166bp and cre negative mice will show nothing other than the IPC at 320bp. When checking for lox P sites, forward and reverse primers for the Cpt1b gene with the start of the primers coming before the insertion points of loxP are used. Control mice with no lox P sites will show one band at 360bp. Floxed mice (mice with target DNA sequence sandwiched between 2 lox P sites) will show one band at 460bp. Heterozygous mice will show one band at 360bp and another band at 460bp.

2.10. Sable Systems Promethion

Mice were put in the Sable Systems International promethion for 1 week. Food and water uptake and respiratory quotient measurements were taken every 5 minutes while in the promethion chamber.

2.11. Statistical Analysis

Data were analyzed by *t* test if normally distributed with an n of at least 8. If data failed D'Agostino-Pearson test for normality or had an n less than 8, the Mann Whitney test was run. Tests were run using GraphPad Prism 7 software. JMP software from SAS was used for the linear regression analysis. The *P* value was set at <0.05 a priori.

Results

When mitochondrial fatty acid oxidation is inhibited in skeletal muscle by knocking out *Cpt1b*, the expression of genes involved in mitochondrial fatty acid oxidation is expected to be upregulated in skeletal muscle. This model would also suggest a build-up of lipid in skeletal muscle. To confirm these expectations, the expression of genes involved in mitochondrial fatty acid oxidation, transport, binding and storage were all measured.

3.1. Cpt1b Deficiency Encapsulates a Model of Lipid Accumulation and FAO Impairment. Increase in the Release of Fatty Acids in Circulation

Impaired fatty acid oxidation in skeletal muscle was achieved by knocking out *Cpt1b*, the rate-limiting enzyme of the long-chain fatty acid beta-oxidation (FAO) pathway in muscle mitochondria. Expression of genes involved in mitochondrial fatty acid oxidation, Hydroxyacyl-CoA dehydrogenase and Enoyl-CoA hydratase 1 (*Hadha* and *Ech1*), were significantly elevated in the gastrocnemius of A^Y:Cpt1b$^{m-/-}$ mice relative to control mice (Figure 2A). The *Hadha* gene is responsible for constructing part of the enzyme complex referred to as mitochondrial trifunctional protein. This complex consists of 3 enzymes which are all essential for fatty acid oxidation. *Ech1* enzyme functions in the auxiliary step of the fatty acid B-oxidation pathway. In addition to this, expression of genes involved in fatty acid transport (*Cd36* and *Fatp1*), binding (*Fabp3*) and storage (*Plin5*) were also upregulated in the gastrocnemius of A^Y:Cpt1b$^{m-/-}$ mice relative to controls and A^Y mice (Figure 2B and 2C). *CD36*, also known as fatty acid translocase, is responsible for long-chain fatty acid transport in muscle cells. Fatty acid transport protein 1 (*Fatp1*) serves as an enhancer of cellular uptake of long-chain fatty acids. Fatty acid binding protein 3 (*Fabp3*) is believed to participate in uptake, metabolism and transport of long-chain fatty acids. Perilipin-5 (*Plin5*) coats the surface of lipid droplets and serves as a barrier which provides increased storage capacity. Taken together, we believe this data displays skeletal muscle specific ablation of *Cpt1b* as a model of FAO impairment and lipid accumulation in genetically obese A^Y:Cpt1b$^{m-/-}$ mice.

A.)

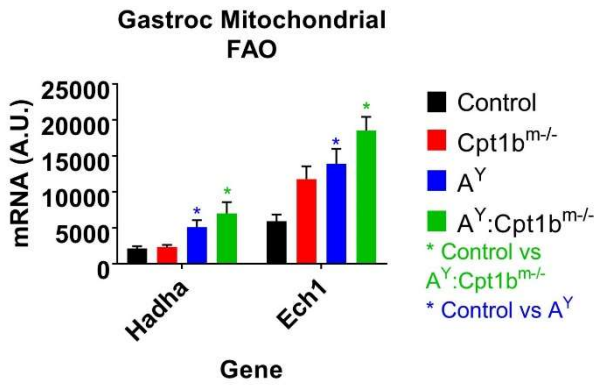

B.)

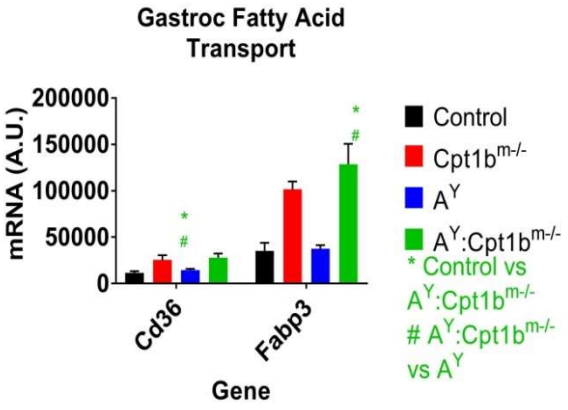

fig cont'd

C.)

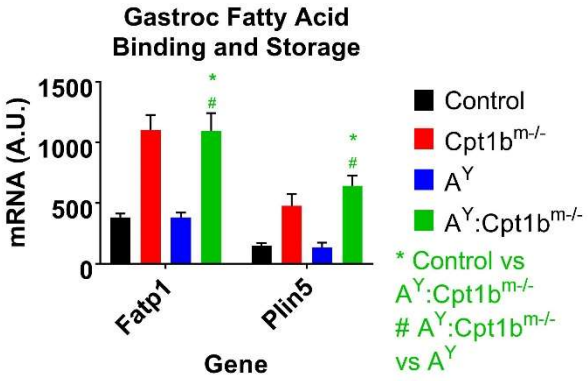

Figure 2. Lipid Accumulation and FAO Impairment in Skeletal Muscle.
A.) Mitochondrial fatty acid oxidation genes are significantly elevated in A^Y and A^Y:Cpt1b$^{m-/-}$ mice relative to control mice. B.) Fatty acid transport, binding and storage genes are upregulated in the gastrocnemius of A^Y:Cpt1b$^{m-/-}$ mice relative to control and A^Y mice. C.) Binding and storage genes are upregulated in the gastrocnemius of A^Y:Cpt1b$^{m-/-}$ mice relative to control and A^Y mice. Significance was set at a $p < 0.05$. n=4-10.

With mitochondrial fatty acid oxidation (FAO) being inhibited in skeletal muscle, we wanted to know if peroxisomal FAO was compensating for the lack of mitochondrial FAO. We were also interested in seeing if other fuel sources were being used in place of fat. We decided to measure the expression of genes involved with peroxisomal fatty acid oxidation and amino acid catabolism.

3.2. Mitochondrial Biogenesis, Peroxisomal FAO and Amino Acid Catabolism are Upregulated in Gastrocnemius of A^Y:Cpt1b$^{m-/-}$ Mice Relative to A^Y Mice

Skeletal muscle of A^Y:Cpt1b$^{m-/-}$ mice appears to become more heavily reliant on peroxisomes for fatty acid oxidation. Peroxisomes are organelles that specialize in the oxidation of a wide variety of fatty acids. Acyl-coenzyme A oxidase 1 (*Acox1*) is an enzyme responsible for performing B-oxidation of fatty acids in the peroxisomes of cells and its expression was found to be upregulated in the gastrocnemius of A^Y:Cpt1b$^{m-/-}$ mice (Figure 3A). Additionally, skeletal muscle of A^Y:Cpt1b$^{m-/-}$ mice appear to use alternative sources of fuel for energy. For example, branched-chain alpha-keto acid dehydrogenase and branched chain amino acid transaminase 2 (*Bckdha1 and Bcat2),* are both involved in the catabolism of branched chain amino acids and are found to be upregulated in the gastrocnemius of A^Y:Cpt1b$^{m-/-}$ mice (Figure 3B).

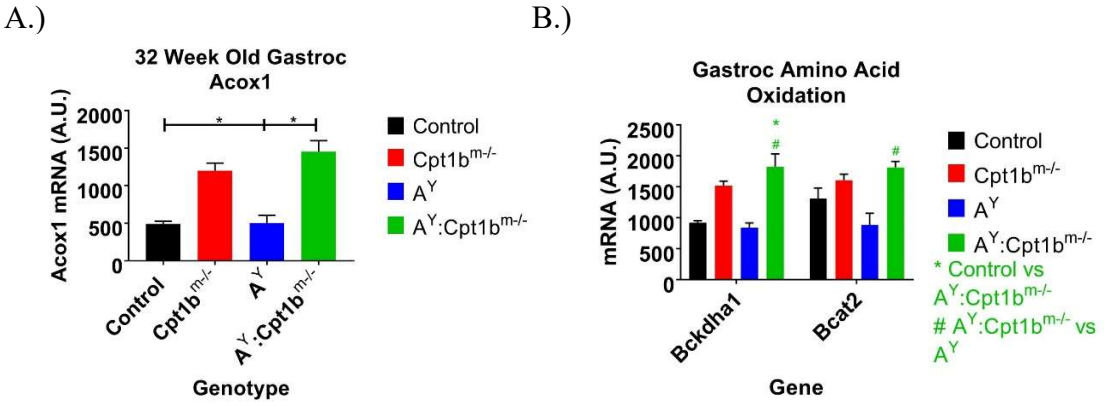

Figure 3. Adaptations Made in Skeletal Muscle
A.) Peroxisomal fatty acid oxidation is significantly elevated in the A^Y:Cpt1b$^{m-/-}$ mice relative to control and A^Y mice. B.) Amino acid oxidation is significantly upregulated in A^Y:Cpt1b$^{m-/-}$ mice relative to controls and A^Y mice. Significance was set at a $p < 0.05$. n=4-10.

We were interested in looking at caloric intake for these mice. Calorimetry data were obtained by housing mice in single-caged promethion chambers for a week long period. Food and water consumption were measured. Cpt1b$^{m-/-}$ mice have previously been shown to eat significantly less relative to control mice when fed a 25% fat diet (Warfel et al., 2017). Therefore, we wanted to see if A^Y:Cpt1b$^{m-/-}$ mice behaved similarly when fed a 25% diet.

3.3. A^Y Mice ate more Food and Drink more Water Relative to A^Y:Cpt1b$^{m-/-}$ Mice

A^Y mice ate significantly more food than the A^Y:Cpt1b$^{m-/-}$ mice (Figure 4A). A^Y mice also consumed significantly more water relative to Control and A^Y:Cpt1b$^{m-/-}$ mice (Figure 4B).

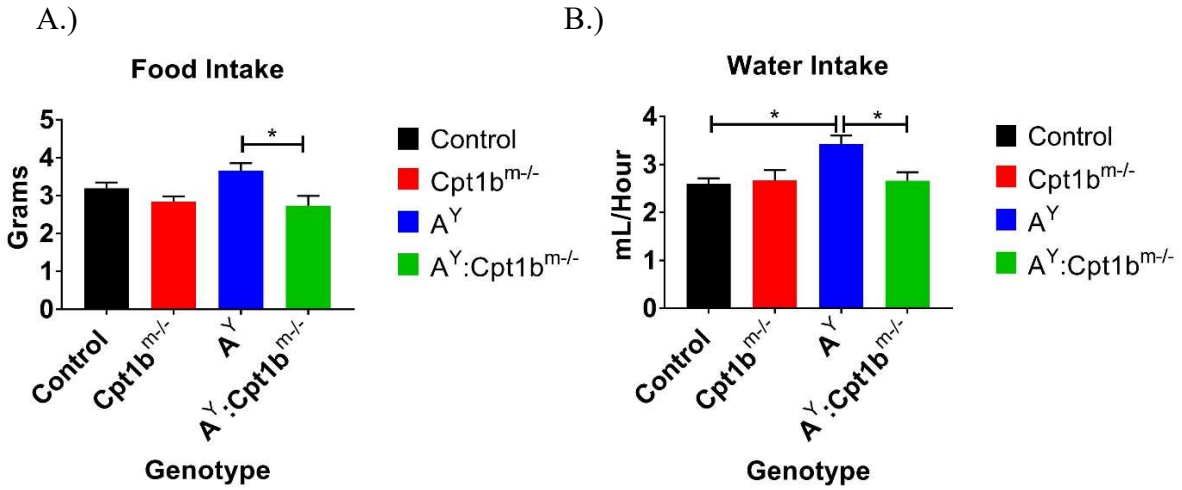

Figure 4. Food and Water Intake
A.) A^Y mice consumed significantly higher amounts of food relative to A^Y:Cpt1b$^{m-/-}$ mice. B.) Water intake for A^Y mice was also significantly higher relative to Control and A^Y:Cpt1b$^{m-/-}$ mice.

Body composition was measured over an 18-week period using a Bruker NMR Minispec. Lean mass was lower in the A^Y:Cpt1b$^{m-/-}$ mice relative to A^Y mice which may explain their decrease in food and water intake. Previously, Cpt1b$^{m-/-}$ mice were shown to have a decrease in food intake relative to controls when fed a 25% fat diet. This decrease in food intake was due to a decrease in lean mass. Cpt1b$^{m-/-}$ had less lean mass; therefore, they were consuming less energy. However, Cpt1b$^{m-/-}$ were shown to maintain control levels for lean mass when fed a 10% diet. It was suggested that skeletal muscle Cpt1b knock out may cause an aversion to fat in the diet (Warfel et al., 2017).

3.4. Compared to A^Y Mice, A^Y:Cpt1b$^{m-/-}$ Mice Have Only Numerically Lower Body Weight, Fat Mass and Lean Mass

Compared to A^Y mice, A^Y:Cpt1b$^{m-/-}$ mice had numerically lower body weights, but differences were not significant (Figure 5A). As the length of the study increased in weeks, this numerical difference increased. Significance was likely not obtained because of the relatively small number of mice and variability. Fat mass for A^Y:Cpt1b$^{m-/-}$ mice had a numerical difference with lower levels than for A^Y mice only for the eighteenth week (Figure 5B). Lean mass for A^Y:Cpt1b$^{m-/-}$ mice was also numerically lower than for A^Y mice from ten through eighteen weeks of the study (Figure 5C). These results indicate that studies with greater numbers of mice may result in statistical differences.

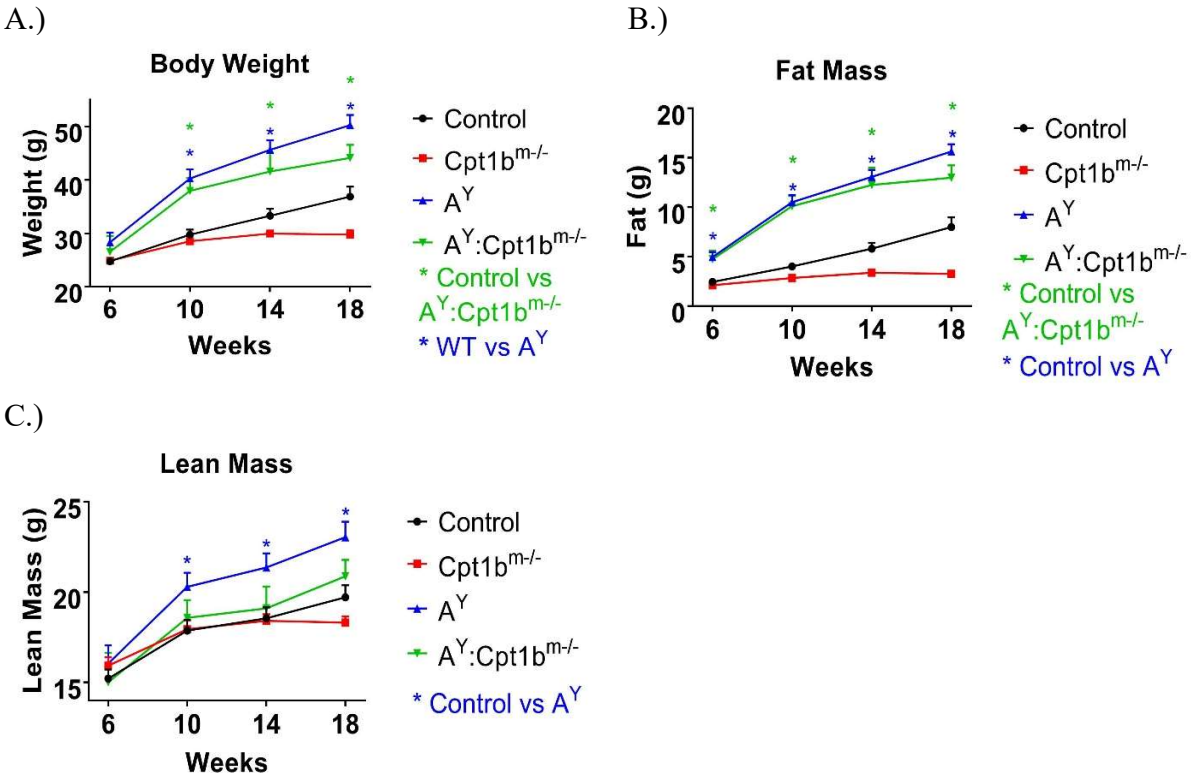

Figure 5. Food and Water Intake
A.) Over an 18 week timeline, A^Y:Cpt1b$^{m-/-}$ mice had numerically lower body weight in comparison to A^Y mice; however, no significant difference was noted between groups. Both

groups were significantly heavier than Control mice. B.) Fat mass for the A^Y:Cpt1b$^{m-/-}$ mice was also numerically below A^Y mice. Both groups had significantly more fat mass than Control mice. C.) Lean mass for the A^Y:Cpt1b$^{m-/-}$ mice was numerically lower than A^Y mice. A^Y mice had significantly more lean mass than Control mice. Significance was set at a $p < 0.05$. n=6-13.

Despite minimal changes in fat mass and body weight for A^Y:Cpt1b$^{m-/-}$ mice relative to A^Y mice, we did find a rather remarkable improvement in glucose clearance and insulin sensitivity. Taken together, these findings suggest a metabolically healthy, yet obese state for the A^Y:Cpt1b$^{m-/-}$ mouse model.

3.5. A^Y:Cpt1b$^{m-/-}$ Mice Have Improved Insulin Resistance and Glucose Clearance Compared to A^Y Mice

Remarkably, despite minimal changes in body weight and composition, A^Y:Cpt1b$^{m-/-}$ mice performed significantly better on glucose clearance and insulin sensitivity tests. At 13-weeks-of-age, A^Y:Cpt1b$^{m-/-}$ mice achieved significantly better results relative to A^Y mice during a glucose tolerance test (GTT) (Figure 6A). Performance during an insulin tolerance test (ITT) at 14-weeks-of-age improved significantly in A^Y:Cpt1b$^{m-/-}$ mice relative to A^Y mice (Figure 6B). A^Y:Cpt1b$^{m-/-}$ mice managed to return to control levels for both tests (GTT and ITT) while blood glucose levels remained elevated in A^Y mice. Insulin levels were checked in 32-week-old mice in the fasted state and A^Y mice had significantly higher fasted insulin levels relative to control and A^Y:Cpt1b$^{m-/-}$ mice. Insulin levels for A^Y:Cpt1b$^{m-/-}$ mice were returned to control levels (Figure 6C).

A.)

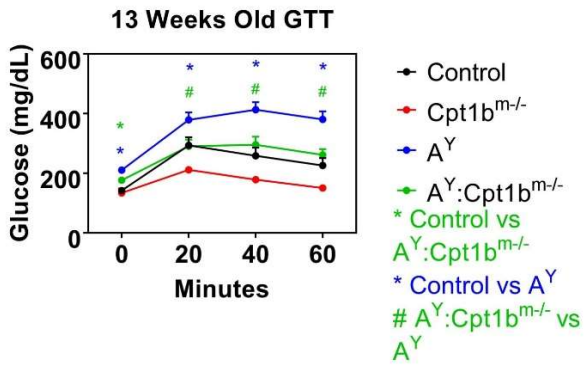

B.)

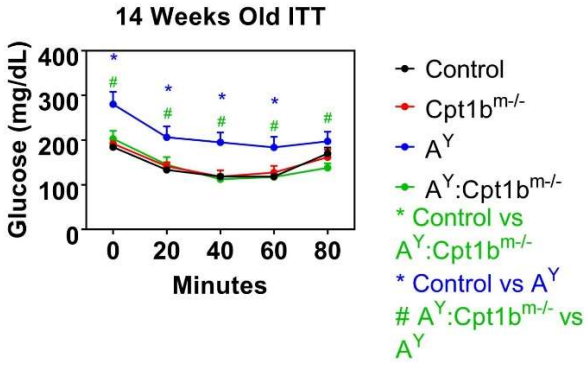

fig cont'd

C.)

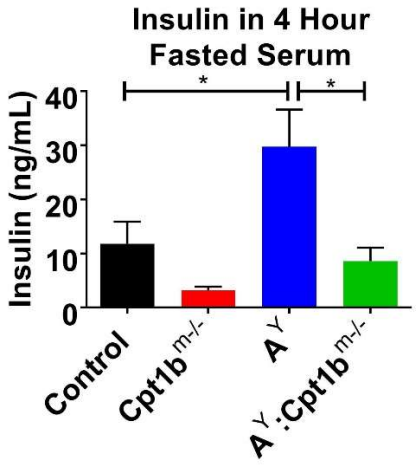

Figure 6. Glucose Tolerance and Insulin Sensitivity
A.) A^{Y}:$Cpt1b^{m-/-}$ mice performed significantly better on glucose tolerance testing (GTT) in comparison to A^{Y} mice at 13 weeks of age. B.) At 14 weeks of age, A^{Y}:$Cpt1b^{m-/-}$ mice performed significantly better during insulin tolerance testing compared to A^{Y} mice. C.) Insulin was measured in serum using an ultra-sensitive mouse insulin ELISA kit. Samples were from 32-week-old mice in the fasted state. A^{Y}:$Cpt1b^{m-/-}$ mice had significantly less circulating insulin in comparison to A^{Y} mice. Significance was set at a $p < 0.05$. n=4-13.

In an attempt to better understand the reason for these improvements in glucose clearance and insulin sensitivity, the expression of *Fgf21* and *Pgc1a* was measured in skeletal muscle. *Fgf21* was measured because it has been shown previously to be contributing to the improvement in glucose clearance and insulin sensitivity seen in the $Cpt1b^{m-/-}$ mice. *Pgc1a* was measured to assess if mitochondrial biogenesis was upregulated in skeletal muscle. If more mitochondria were present, this may offer an explanation for improved glucose clearance.

3.6. A^{Y}:$Cpt1b^{m-/-}$ Mice Have Elevated Fgf21 and Pgc1a in Skeletal Muscle Relative to A^{Y} Mice.

Fibroblast growth factor 21 (*Fgf21*) is elevated in the gastrocnemius of A^{Y}:$Cpt1b^{m-/-}$ mice (Figure 6A). *Fgf21* has been shown as being partially responsible for enhanced glucose clearance in $Cpt1b^{m-/-}$ mice. With a similar result seen in A^{Y}:$Cpt1b^{m-/-}$ mice, we assume *Fgf21* likely plays a role in the insulin sensitizing effect seen in the double mutant mouse model. $Cpt1b^{m-/-}$ mice appear to acclimate to the muscle specific ablation with favorable adaptations such as increased mitochondrial biogenesis. Peroxisome proliferator-activated receptor gamma coactivator 1-alpha, *Pgc1a,* is a transcriptional coactivator that serves as a central inducer in mitochondrial biogenesis and it is significantly elevated in gastrocnemius muscle of A^{Y}:$Cpt1b^{m-/-}$ mice relative to control and A^{Y} mice (Figure 7B).

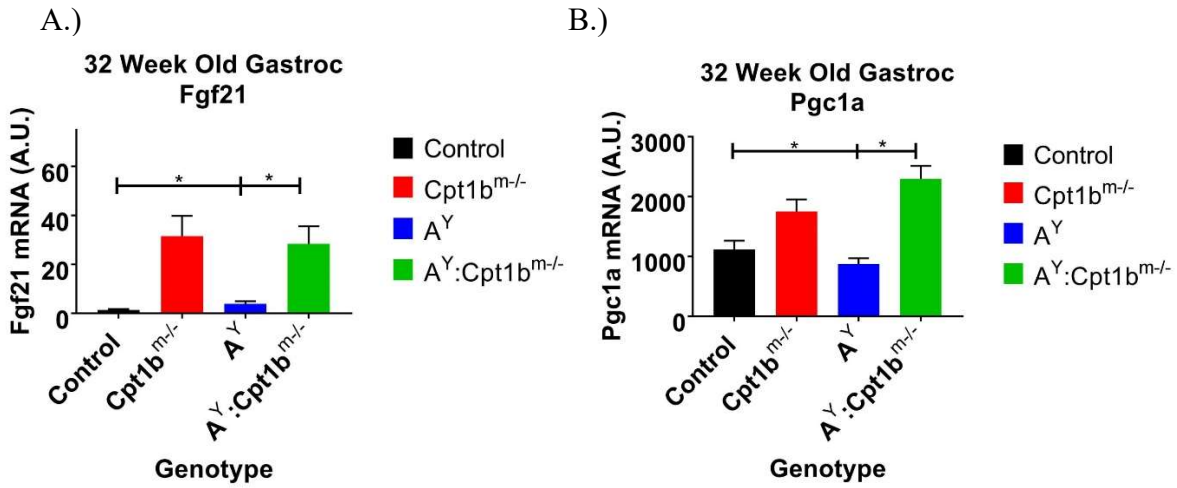

Figure 7. Skeletal Muscle Fgf21 and Pgc1a
A.) At 32 weeks of age, *Fgf21* expression in gastrocnemius is significantly elevated in A^Y:Cpt1b$^{m-/-}$ mice relative to Control and A^Y mice. B.) Mitochondrial biogenesis is significantly upregulated in the A^Y:Cpt1b$^{m-/-}$ mice relative to control and A^Y mice. Significance was set at a $p < 0.05$. n=4-9.

In addition to improving glucose clearance and insulin sensitivity, *Fgf21* is known for having a paradoxical effect in which its levels are elevated in the circulation of obese mice. Some have proposed obesity as an *Fgf21* resistant state. We decided to evaluate this in our mice by using an *Fgf21* Elisa kit to measure levels in fed serum. Since levels in the A^Y:Cpt1b$^{m-/-}$ mice were found to be numerically lower than A^Y levels, the skeletal muscle *Cpt1b* knock out may be responsible for lower levels in circulation and suggestive of improved overall utilization of *Fgf21.*

3.7. Fgf21 is Elevated in Serum of 32 Week Old A^Y:Cpt1b$^{m-/-}$ Mice in the Fed State Relative to Control Mice, but Less than A^Y Mice

Fgf21 was found to be significantly elevated in the serum of A^Y mice in the fed state relative to control mice (Figure 8). This elevation in serum may be indicative of *Fgf21* resistance in the genetically obese A^Y mice. As seen in Figure 7, the *Fgf21* in fed serum of A^Y mice does not appear to be coming from skeletal muscle. Rather, the primary source of *Fgf21* in A^Y mice appears to be from hepatic production. *Fgf21* was elevated in the gastrocnemius and liver for A^Y:Cpt1b$^{m-/-}$ mice; however, *Fgf21* in fed serum was not significantly elevated in A^Y:Cpt1b$^{m-/-}$ mice. Therefore, muscle specific knockout of *Cpt1b* may help avoid *Fgf21* resistance and promote insulin sensitivity.

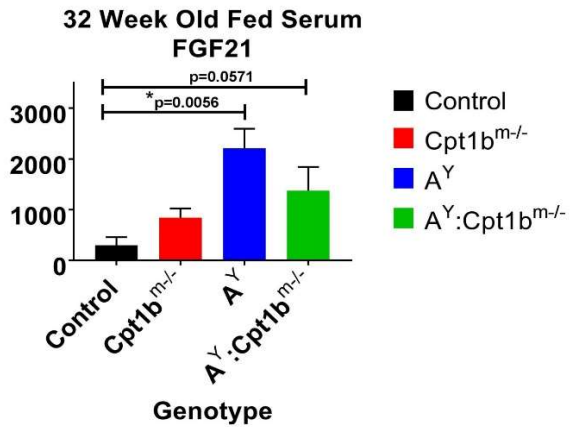

Figure 8. *Fgf21* in Circulation
Fgf21 is increased in serum of 32 week old A^Y:Cpt1b$^{m-/-}$ mice relative to Control, but decreased relative to A^Y mice, which could suggest *Fgf21* resistance in A^Y mice, while not in A^Y:Cpt1b$^{m-/-}$ mice. Significance was set at a $p < 0.05$. n=3-9.

While improvements in glucose clearance and insulin sensitivity are heavily notable in the A^Y:Cpt1b$^{m-/-}$ mice, we also observed a significant decrease in their liver weights relative to A^Y mice. This decrease in weight could be suggestive of improved hepatic health relative to A^Y mice. Further investigation will be needed to confirm this assumption.

3.8. Liver Weight is Decreased in A^Y:Cpt1b$^{m-/-}$ Mice Relative to A^Y Mice

Liver weights were drastically decreased in A^Y:Cpt1b$^{m-/-}$ mice relative to A^Y mice (Figure 9). Differences in weights are further discussed in Figure 10.

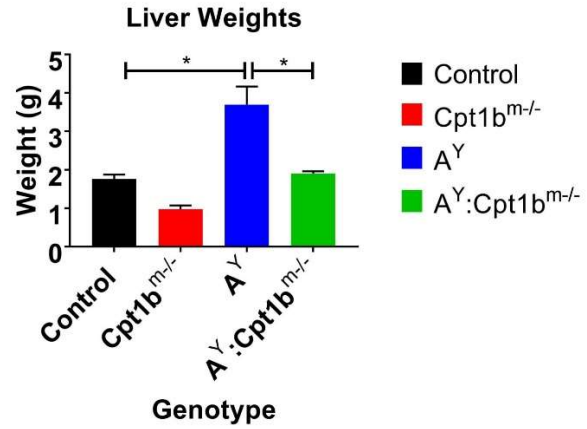

Figure 9. Liver Weight
Liver weights of A^Y:Cpt1b$^{m-/-}$ mice were significantly lower than liver weights of A^Y mice. Significance was set at a $p < 0.05$. n=4-10.

With liver weight being significantly lower in A^Y:Cpt1b$^{m-/-}$ mice relative to A^Y mice, we began to wonder what was accounting for this difference in weight. Since liver is an important

storage site for glycogen, we decided to assess hepatic glycogen levels to see if storage was depleted in the livers of A^Y:Cpt1b$^{m-/-}$ mice relative to A^Y mice. We also assumed the liver may be compensating for the loss of fatty acid oxidation in the muscle and have less ectopic fat as a result. We decided to measure hepatic triglyceride levels. Additionally, lipid droplets were viewed in liver samples that were embedded in paraffin and sectioned and stained with H&E at the Cell Biology and Bioimaging Core Facility at Pennington Biomedical Research Center.

3.9. Liver Glycogen and Triglycerides are Numerically Decreased in A^Y:Cpt1b$^{m-/-}$ Mice Relative to A^Y Mice According to Chemical Analyses, but Histology Samples Demonstrate Lower Fat Mass

Triglycerides in the liver of 32-week-old mice were significantly elevated in A^Y mice relative to Control. Triglyceride levels in A^Y:Cpt1b$^{m-/-}$ mice were not significantly elevated relative to Control mice; however, the levels were not significantly less than A^Y mice. Triglycerides in the liver of A^Y:Cpt1b$^{m-/-}$ mice were numerically lower than for A^Y mice with the p value equaling 0.1531 (Figure 10A). Hepatic glycogen levels followed a similar trend between A^Y and A^Y:Cpt1b$^{m-/-}$ mice with A^Y:Cpt1b$^{m-/-}$ mice having lower glycogen amounts than A^Y mice without reaching significance (Figure 10B). The p value between these two groups was p = 0.0952. While neither hepatic triglyceride or glycogen levels showed statistically significant differences between A^Y and A^Y:Cpt1b$^{m-/-}$ mice, A^Y:Cpt1b$^{m-/-}$ mice had numerically lower amounts and these numerical differences combined to result in a statistically significant difference in liver weight. Histology samples also show less ectopic lipid in the livers of A^Y:Cpt1b$^{m-/-}$ mice relative to A^Y mice (Figure 10C). Triglyceride content provides non-conclusive evidence that fats are decreased in A^Y:Cpt1b$^{m-/-}$ liver relative to A^Y liver; however, other tissue levels such as white adipose, cholesterol and ceramide fat species still need to be quantified.

A.)

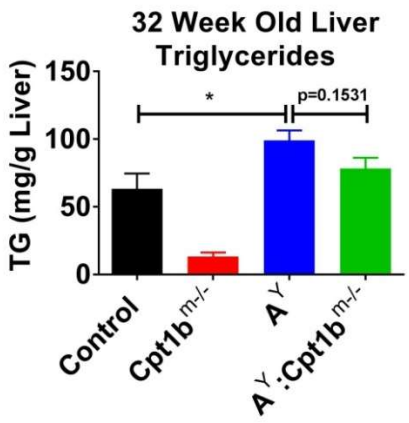

B.)

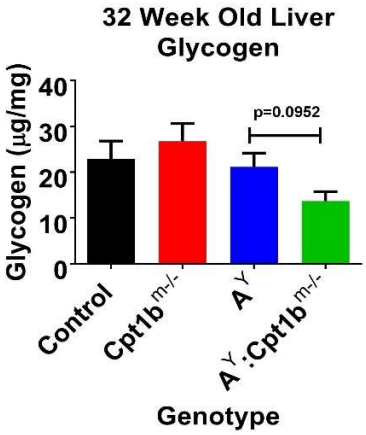

fig cont'd

C.)

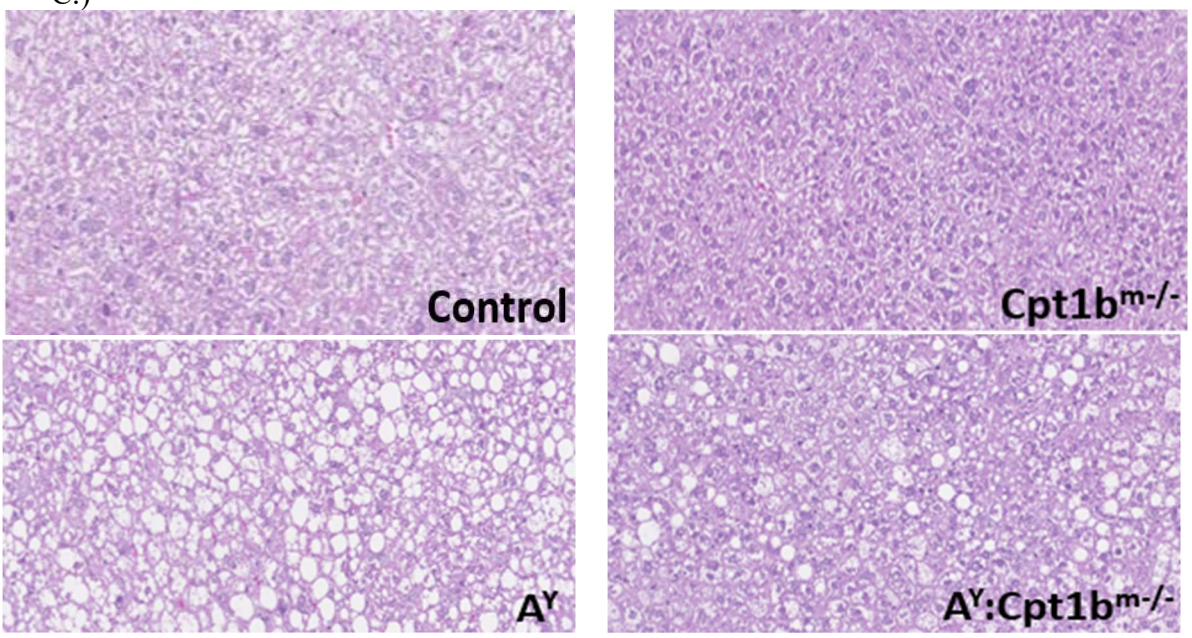

Figure 10. Hepatic Triglycerides and Glycogen Levels and Histology Images
A.) Liver triglycerides levels were numerically lower in the livers of A^{Y}:$Cpt1b^{m-/-}$ mice when compared to liver triglycerides of A^{Y} mice; however, there was no statistical significance. B.) Liver glycogen levels were also lower in A^{Y}:$Cpt1b^{m-/-}$ mice when compared to liver glycogen levels of A^{Y} mice; however, there was also no statistical significance. C.) Liver histology images (5x magnification) show more ectopic fat accumulation in the A^{Y} mice relative to the A^{Y}:$Cpt1b^{m-/-}$ mice. Significance was set at a $p < 0.05$. n=3-8.

While triglyceride and glycogen levels were numerically lower in A^{Y}:$Cpt1b^{m-/-}$ mice relative to A^{Y} mice, we did not think this was enough to account for the difference in liver weights. Therefore, we decided to assess hepatic fluid levels as well.

3.10. Liver Contains Less Fluid Mass in A^{Y}:$Cpt1b^{m-/-}$ Mice Relative to A^{Y} Mice

In addition to hepatic triglyceride and glycogen levels being numerically lower in A^{Y}:$Cpt1b^{m-/-}$ mice compared to A^{Y} mice, hepatic fluid levels were significantly greater for A^{Y} mice (Figure 11A). A correlation plot between fluid and triglyceride + glycogen content generated an R^2 value of 0.5; therefore, numerically greater triglyceride and glycogen amounts appear to promote greater fluid retention (Figure 11B).

A.)

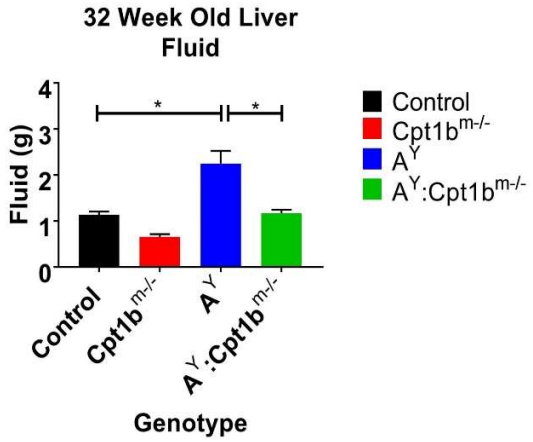

B.)

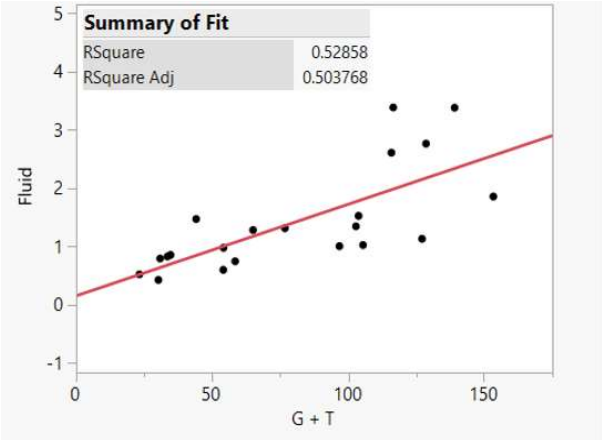

Figure 11. Hepatic Fluid and Fluid Retention Correlation Plot
A.) Liver fluid levels of A^Y:Cpt1b$^{m-/-}$ mice were significantly less than liver fluid levels of A^Y mice. B.) Correlation plot between triglycerides + glycogen and fluid had a R^2 value of 0.5. Significance was set at a $p < 0.05$. n=4-10.

As seen previously in Figure 10C, histology images seem to reveal lower amounts of ectopic fat in the livers of A^Y:Cpt1b$^{m-/-}$ mice relative to A^Y mice. To further assess this finding, we decided to measure the expression of several genes involved in fatty acid synthesis.

3.11. Fatty Acid Synthesis Pathways Are Decreased in the Liver of A^Y:Cpt1b$^{m-/-}$ Mice Relative to A^Y Mice

Expression of enzymes involved in fatty acid synthesis was significantly upregulated in the liver of A^Y mice relative to Control and A^Y:Cpt1b$^{m-/-}$ mice at 16-weeks-of-age. Acetyl-CoA carboxylase (*Acaca*), the enzyme responsible for catalyzing the carboxylation of acetyl-CoA to malonyl-CoA, is significantly upregulated in the liver of A^Y mice relative to Control mice at 16-weeks-of-age. It is also increased in A^Y:Cpt1b$^{m-/-}$ mice relative to Control mice; however, A^Y:Cpt1b$^{m-/-}$ expression trends less than A^Y mice (Figure 12A). Fatty acid synthase (*Fasn*), the enzyme involved with catalyzing the synthesis of palmitate from acetyl-CoA and malonyl-CoA, is significantly upregulated in the livers of A^Y mice relative to Control and A^Y:Cpt1b$^{m-/-}$ mice at 16-weeks-of-age (Figure 12B). Stearoyl-CoA desaturase (*Scd1*), the enzyme primarily responsible for the synthesis of oleic acid, is upregulated in the liver of A^Y mice relative to Control and A^Y:Cpt1b$^{m-/-}$ mice at 16-weeks-of-age (Figure 12C). At 32-weeks-of-age, expression of enzymes involved in fatty acid synthesis (*Fasn* and *Scd1*) were numerically greater in livers of A^Y mice relative to Control and A^Y:Cpt1b$^{m-/-}$ mice (Figure 12D and 12E). However, *Acaca* was significantly elevated in A^Y mice relative to Control mice, but only numerically higher than A^Y:Cpt1b$^{m-/-}$ mice at 32-weeks-of-age (Figure 12F). Expression of these enzymes appears to increase with age for all groups with upregulation occurring earlier in A^Y mice. Expression appears to remain higher in A^Y mice relative to all groups despite age. However, for the most part, the higher amounts were not significantly different. While not significant (likely due to low n with relatively high variability), these data may still be suggestive of elevated fatty acid

synthesis in the livers of A^Y mice relative to A^Y:Cpt1b$^{m-/-}$ mice. Additional studies with a larger number of mice per group are needed to confirm elevated levels in A^Y mice at 32 weeks of age.

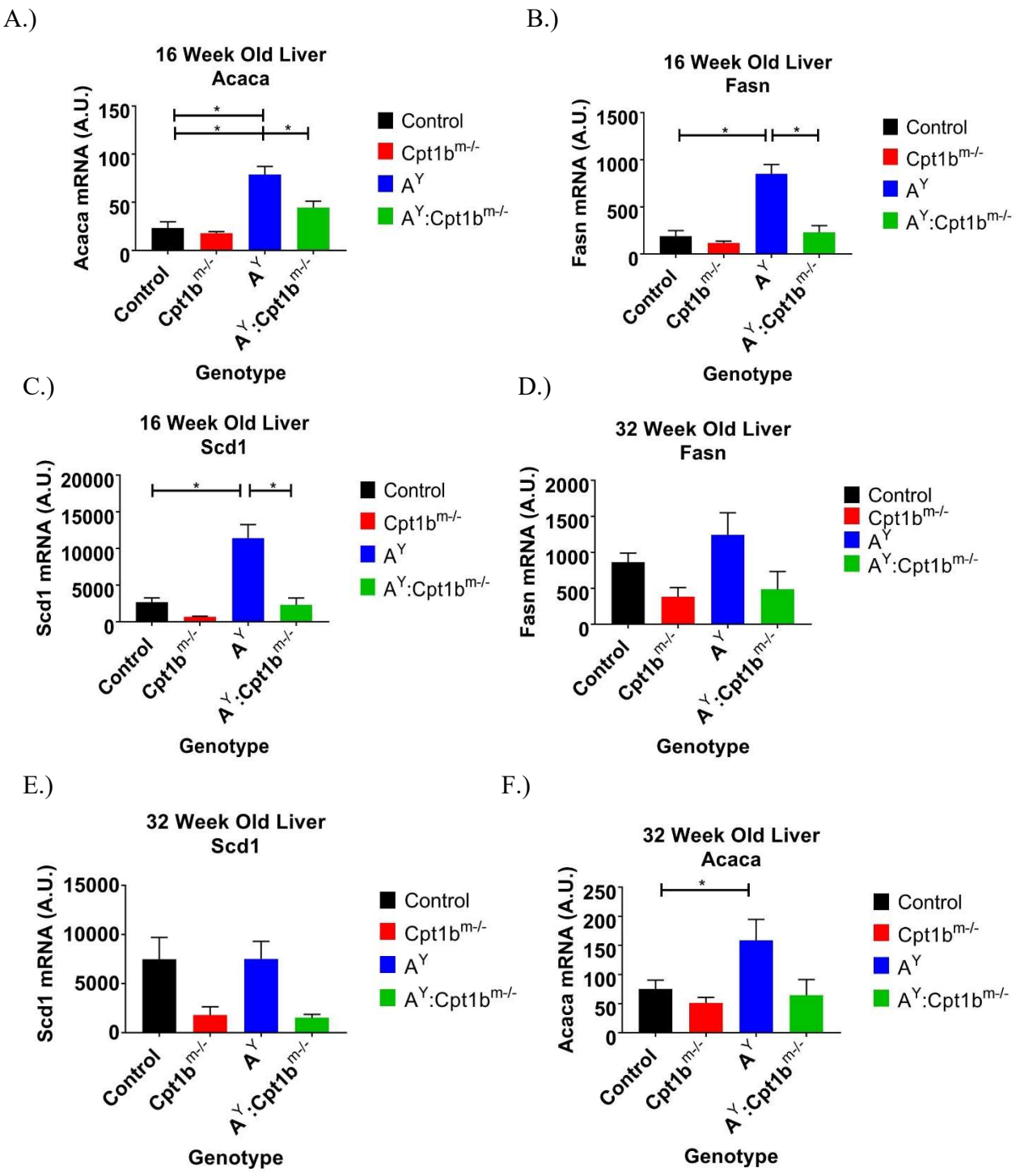

Figure 12. Hepatic Fatty Acid Synthesis
A.) Acetyl-CoA carboxylase alpha (*Acaca*) is significantly elevated in livers of 16-week-old A^Y mice relative to Control and A^Y:Cpt1b$^{m-/-}$ mice. *Acaca* is also significantly elevated in

A^Y:Cpt1b$^{m-/-}$ mice relative to Control. B.) Fatty acid synthase (*Fasn*) is significantly elevated in livers of 16-week-old A^Y mice relative to Control and A^Y:Cpt1b$^{m-/-}$ mice. C.) Stearoyl-CoA Desaturase (*Scd1*) is significantly elevated in livers of 16-week-old A^Y mice relative to Control and A^Y:Cpt1b$^{m-/-}$ mice. These data may be suggestive of elevated fatty acid synthesis in the livers of A^Y mice relative to A^Y:Cpt1b$^{m-/-}$ mice. D.) Hepatic *Fasn* was numerically higher in A^Y mice relative to control and A^Y:Cpt1b$^{m-/-}$ at 32 weeks of age. E.) Hepatic *Scd1* was numerically higher in A^Y mice relative to control and A^Y:Cpt1b$^{m-/-}$ at 32 weeks of age. F.) *Acaca* is significantly elevated in the livers of 32-week-old A^Y mice relative to Control mice and is numerically higher in A^Y mice relative to A^Y:Cpt1b$^{m-/-}$ mice. Significance was set at a $p < 0.05$. n=4-9.

Additionally, we wanted to check if mitochondrial and peroxisomal fatty acid oxidation was upregulated in the livers of A^Y:Cpt1b$^{m-/-}$ mice relative to A^Y mice. We decided to measure hepatic gene expression of genes involved with mitochondrial and peroxisomal fatty acid oxidation.

3.12. Hepatic Mitochondrial and Peroxisomal Fatty Acid Oxidation is Increased in the Liver of A^Y:Cpt1b$^{m-/-}$ Mice Relative to A^Y Mice

A.)

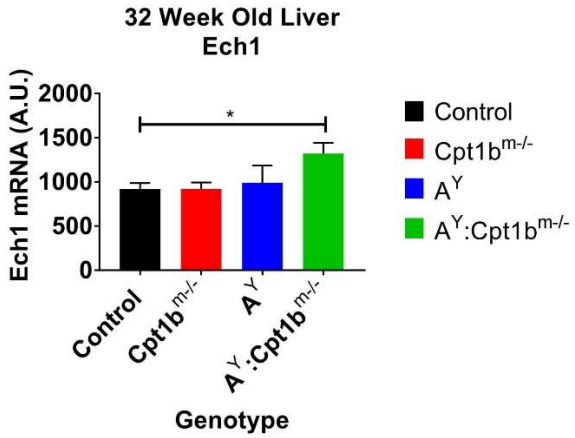

B.)

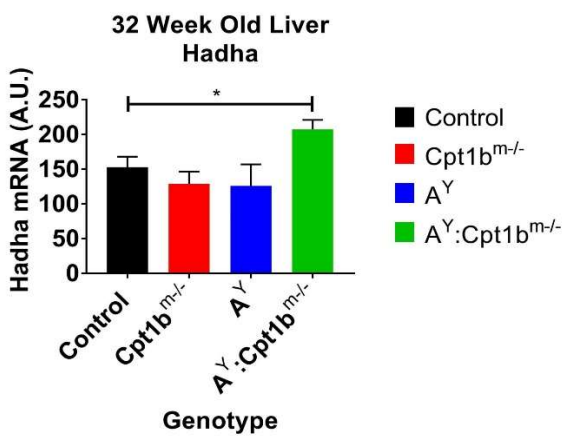

C.)

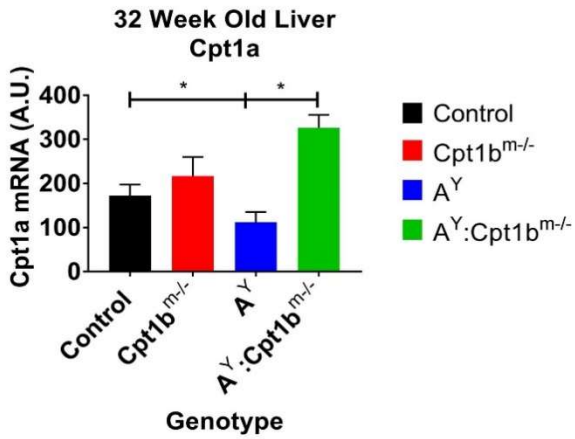

D.)

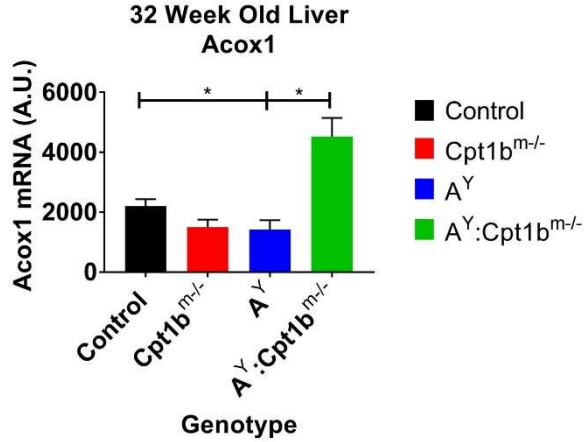

Figure 13. Hepatic Fatty Acid Oxidation
A.) *Ech1* was significantly upregulated in the liver of A^Y:Cpt1b$^{m-/-}$ mice relative to Control mice. B.) *Hadha* was significantly upregulated in the liver of A^Y:Cpt1b$^{m-/-}$ mice relative to Control mice. C.) *Cpt1a* was found to be was found to be significantly elevated in the liver of A^Y:Cpt1b$^{m-/-}$ mice relative to Control and A^Y mice. D.) *Acox1*, involved with peroxisomal fatty acid oxidation, was also found to be significantly elevated in the liver of A^Y:Cpt1b$^{m-/-}$ mice relative to Control and A^Y mice .

Mitochondrial and peroxisomal fatty acid oxidation may be elevated in the liver of A^Y:Cpt1b$^{m-/-}$ mice to compensate for the inhibition of mitochondrial fatty acid oxidation in skeletal muscle. Respiratory quotient (RQ) data obtained from the promethion chambers show A^Y:Cpt1b$^{m-/-}$ mice maintaining lower RQ's relative to A^Y mice (Figure 14). This RQ data appears to indicate that A^Y:Cpt1b$^{m-/-}$ mice are burning more fat for fuel relative to A^Y mice. Additionally, genes involved with mitochondrial and peroxisomal fatty acids were found to be up in the liver of A^Y:Cpt1b$^{m-/-}$ mice. Taken together, these data may suggest increased reliance on fat for fuel and consequentially reduced ectopic fat in the liver of A^Y:Cpt1b$^{m-/-}$ mice.

3.13. Respiratory Quotient is Lower for A^Y:Cpt1b$^{m-/-}$ Mice Relative to A^Y Mice

A.) B.)

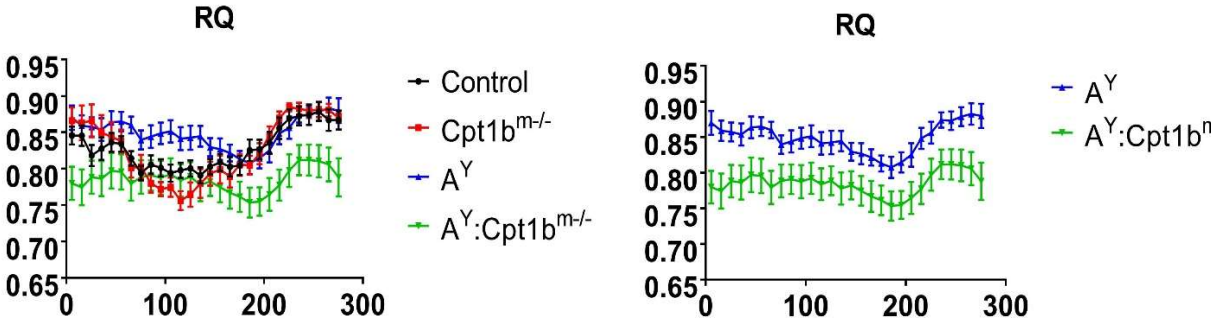

Figure 14. Respiratory Quotient
A.) The respiratory quotient for A^Y:Cpt1b$^{m-/-}$ mice remains lower than that of A^Y mice, suggesting a higher dependence on fat as a fuel source. B.) This graph displays only RQ's of A^Y and A^Y:Cpt1b$^{m-/-}$ mice.

In addition to a lower RQ and increased hepatic mitochondrial and peroxisomal fatty acid oxidation, hepatic gluconeogenesis was also found to be elevated in the liver of A^Y:Cpt1b$^{m-/-}$ mice.

3.14. Based on an Increase in Amounts of the Major Regulatory Gene for Gluconeogenesis, This Pathway for Glucose Synthesis Appears to be Increased in the Liver of A^Y:Cpt1b$^{m-/-}$ Mice Relative to A^Y Mice

Noteworthy, phosphoenolpyruvate carboxykinase (*Pck1*), the major regulatory gluconeogenic enzyme, is significantly upregulated in 32-week-old liver of A^Y:Cpt1b$^{m-/-}$ relative to Control and A^Y mice (Figure 15). The reason for this is unknown but may indicate that they

are making more glucose to supply it for skeletal muscle. Additionally, the A^Y:Cpt1b$^{m-/-}$ mice may also have an increased need for glucose for energy.

A).

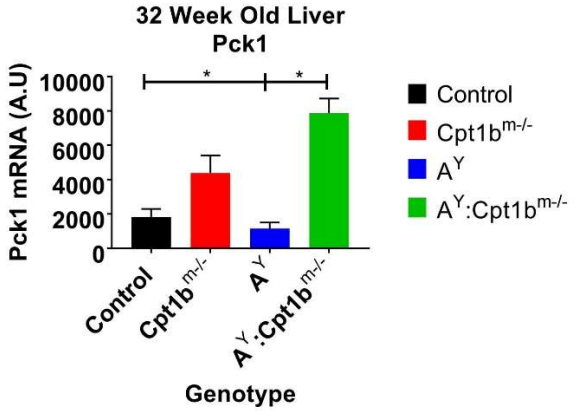

Figure 15. Hepatic Gluconeogenesis
A.) Gluconeogenesis appears to be significantly elevated in the livers of A^Y:Cpt1b$^{m-/-}$ mice in comparison to A^Y mice. Significance was set at a $p < 0.05$. n=4-6.

Triglycerides were significantly reduced in the serum of A^Y:Cpt1b$^{m-/-}$ mice relative to A^Y mice. Hepatic triglycerides were not significantly different between groups (Figure 10A); however, significantly less triglycerides are released into circulation for A^Y:Cpt1b$^{m-/-}$ mice relative to A^Y mice. Previous research has shown *Gdf15* to increase the release of hepatic triglycerides into circulation (Luan et al., 2019). Expression of *Gdf15* was found to be upregulated in the liver of A^Y mice relative to A^Y:Cpt1b$^{m-/-}$ mice and may explain the significant increase in circulating triglycerides.

3.15. Gdf15 is Upregulated in the Liver of A^Y Mice Relative to All Groups and May Explain the Increase in the Release of Fatty Acids in Circulation

At 16-weeks-of-age growth differentiation factor 15 (*Gdf15*) was significantly elevated in A^Y mice relative to Control and A^Y:Cpt1b$^{m-/-}$ mice (Figure 16A). At 32-weeks-of-age, *Gdf15* was numerically higher than Control (p=0.054) and A^Y:Cpt1b$^{m-/-}$ mice; however, no significance was noted (Figure 16B). Triglycerides in serum of mice fasted for 4-hours were significantly higher in A^Y mice relative to Control and A^Y:Cpt1b$^{m-/-}$ mice. Levels for A^Y:Cpt1b$^{m-/-}$ mice were significantly lower than for Control mice (Figure 16C). The elevated expression of hepatic *Gdf15* in A^Y mice may be partially responsible for the increase in triglyceride circulation.

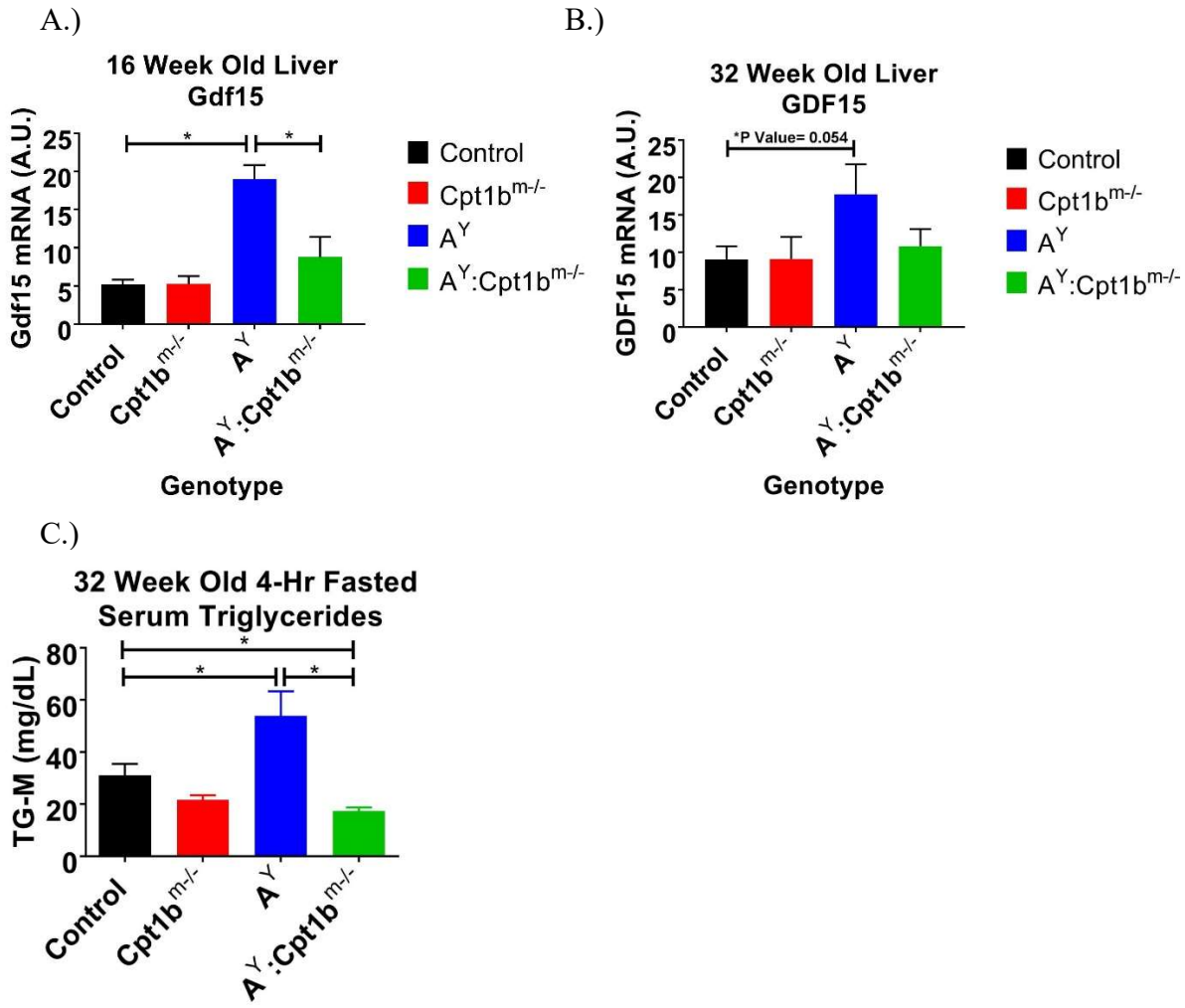

Figure 16. Hepatic *Gdf15* and Triglycerides in Circulation
A.) Hepatic *Gdf15* expression in A^Y mice is significantly higher than for Control and A^Y:Cpt1b$^{m-/-}$ mice at 16-weeks of age. B.) Hepatic *Gdf15* expression in A^Y mice is numerically higher than for Control and A^Y:Cpt1b$^{m-/-}$ mice at 32-weeks of age. C.) Triglycerides in serum of mice fasted for 4 hours was significantly lower in A^Y:Cpt1b$^{m-/-}$ mice relative to Control and A^Y mice. Significance was set at a $p < 0.05$. n=4-10.

Table 2. Summary of Results.

Measurements	Results
Promethion Data	**A^Y:Cpt1b$^{m-/-}$ Relative to A^Y**
Food Intake	↓
Water Intake	↓
Respiratory Quotient	↓
Muscle Metabolism mRNA	**A^Y:Cpt1b$^{m-/-}$ Relative to A^Y**
Mitochondrial Fatty Acid Oxidation	↑
Fatty Acid Transport, Binding and Storage	↑
Peroxisomal Fatty Acid Oxidation	↑
Amino Acid Catabolism	↑
Mitochondrial Biogenesis	↑
Fgf21	↑
Hepatic mRNA	**A^Y:Cpt1b$^{m-/-}$ Relative to A^Y**
Gluconeogenesis	↑
Gdf15	↓
Fatty Acid Oxidation	↑
Fatty Acid Synthesis	↓
Metabolic Health	**A^Y:Cpt1b$^{m-/-}$ Relative to A^Y**
Improved Glucose Utilization	✓
Improved Insulin Sensitivity	✓
Decreased Body Weight	✗
Decreased Fat Mass	✗
Decreased Lean Mass	✓

table cont'd.

Measurements	Results
Promethion Data	**A^Y:Cpt1b$^{m-/-}$ Relative to A^Y**
Fgf21	↓
Insulin	↓
Triglycerides	↓
Liver	**A^Y:Cpt1b$^{m-/-}$ Relative to A^Y**
Weight	↓
Triglycerides	↓
Glycogen	↓
Fluid	↓

Discussion

4.1. Improvements in Metabolic Health

Inhibition of long chain fatty acid B-oxidation in the mitochondria of skeletal muscle has rescued the metabolic health of genetically obese A^Y mice. Despite minimal changes in fat mass and body weight, A^Y:Cpt1b$^{m-/-}$ mice drastically improve their performance during glucose tolerance testing and insulin tolerance testing. In comparison to A^Y mice, A^Y:Cpt1b$^{m-/-}$ mice have significantly lower amounts of insulin and triglycerides in the circulation of 32-week-old mice in the fasted state. Gene expression for enzymes involved with fatty acid synthesis were down in the livers of A^Y:Cpt1b$^{m-/-}$ mice relative to A^Y mice and may explain the decrease in circulating triglycerides. Additionally, hepatic triglycerides were numerically lower in A^Y:Cpt1b$^{m-/-}$ mice relative to A^Y mice and histology liver images appear to show a decrease in ectopic lipid accumulation for A^Y:Cpt1b$^{m-/-}$ mice. Liver weights for A^Y:Cpt1b$^{m-/-}$ mice were significantly lower than that of A^Y mice. Taken together, these data are suggestive of improved metabolic and hepatic health in A^Y:Cpt1b$^{m-/-}$ mice even though there were minimal changes in fat mass and body weight. The reason why Cpt1b$^{m-/-}$ mice exhibit a leaner phenotype is still under investigation; however, Agouti mice must be blocked from having the effects of these anorectic factors. The blocking may be due to the presence of the agouti protein. Further investigation is needed in order to unmask the lingering questions of why Cpt1b$^{m-/-}$ mice become leaner when long chain fatty acid B-oxidation is inhibited in skeletal muscle mitochondria and what is preventing Agouti mice from doing the same.

4.2. Modifications Occurring in Skeletal Muscle of A^Y:Cpt1b$^{m-/-}$ Mice

Skeletal muscle-specific *Cpt1b* knock out in genetically obese A^Y mice appear to strongly embody a model of lipid aggregation and FAO impairment. Expression of genes involved with fatty acid binding (*Fabp3*), lipid droplet forming (*Plin5*) and fatty acid transport (*Cd36, Fatp1*) were all significantly increased in gastrocnemius muscle of A^Y:Cpt1b$^{m-/-}$ mice. Expression of *Hadha* and *Ech1*, genes associated with mitochondrial FAO, were significantly upregulated in A^Y:Cpt1b$^{m-/-}$ mice relative to Control mice. Furthermore, peroxisomal FAO appears to compensate for impairment of mitochondrial FAO in muscle. Acyl-CoA oxidase 1 (*Acox1)*, a peroxisomal FAO gene, was found to be upregulated in A^Y:Cpt1b$^{m-/-}$ mice. Inhibition of fatty acid oxidation appears to result in usage of alternative fuel sources in muscle. *Bckdha and Bcat2,* genes associated with mitochondrial branched-chain amino acid cycle, were elevated in the gastrocnemius of A^Y:Cpt1b$^{m-/-}$ mice.

As seen previously in muscle of Cpt1b$^{m-/-}$ mice, muscle of A^Y:Cpt1b$^{m-/-}$ mice appear to undergo a plethora of effects that could be induced by an energy deficit signal elicited from inhibition of B-oxidation. AMP-activated protein kinase (AMPK) is a sensor of cellular energy status that becomes activated with a high ratio of AMP:ATP in the cell. AMPK is a promoter of glucose uptake, fatty acid oxidation, mitochondrial biogenesis and insulin sensitivity (O'Neill, 2013). Previous work with Cpt1b$^{m-/-}$ mice found a significant increase in the phosphorylation of the α-subunit of AMPK at Thr-172 relative to control mice. Additionally, AMPK target peroxisome proliferator-activated receptor gamma coactivator 1-alpha (*Pgc1α*) was found to be robustly elevated in both red and white muscles (S. E. Wicks et al., 2015). *Pgc1α* is often accredited as a master in the regulation of mitochondrial biogenesis and was elevated in

A^Y:Cpt1b$^{m-/-}$ mice. This suggests that there may be more mitochondria in the skeletal muscle of mice with the skeletal-muscle specific *Cpt1b* knock out. Increases in the number of mitochondria in skeletal muscle may be partially responsible for improved glucose utilization. While *Pgc1α* expression in gastrocnemius was found to be elevated in both Cpt1b$^{m-/-}$ and A^Y:Cpt1b$^{m-/-}$ mice, phosphorylation of the α-subunit of AMPK at Thr-172 was never measured in A^Y:Cpt1b$^{m-/-}$ mice. Given that A^Y:Cpt1b$^{m-/-}$ mice have increased mitochondrial biogenesis in gastrocnemius, improved glucose clearance and enhanced insulin sensitivity, we hypothesize the phosphorylation of the α-subunit of AMPK at Thr-172 would follow a similar pattern in A^Y:Cpt1b$^{m-/-}$ mice relative to Cpt1b$^{m-/-}$ mice. Additional work will be needed to confirm this hypothesis.

4.3. The Impact of *Fgf21*

Expression of *Fgf21* was elevated in the muscle of A^Y:Cpt1b$^{m-/-}$ mice. A double knockout mouse model of *Cpt1b* and *Fgf21* showed a partial negation in improved glucose utilization in comparison to *Cpt1b* knock outs (Vandanmagsar et al., 2016). *Fgf21* may be somewhat responsible for the increase in glucose utilization when *Cpt1b* is knocked out in skeletal muscle. However, there are definitely other factors contributing to these improvements and the relevance of the physiological effects *Fgf21* has on improved metabolic health in skeletal-muscle specific *Cpt1b* knock out mice may be questionable. Transcriptomics and proteomic analyses could potentially identify other contenders contributing to the improvements on metabolic health in skeletal-muscle specific *Cpt1b* knock out mice.

Fgf21 in the serum of mice in the fed state was significantly elevated for A^Y mice relative to Control mice, but there was not statistical significance between A^Y:Cpt1b$^{m-/-}$ mice and Control mice. Elevated *Fgf21* serum levels have been observed in genetically and diet-induced obese mouse models. One study suggested that obesity is an *Fgf21*-resistant state. Their study evaluated the response of obese mice to administration of exogenous *Fgf21* and noted a significantly reduced signaling response in diet-induced obese mice. They concluded by stating diet-induced obesity results in elevated endogenous *Fgf21* levels and poor response to administration of exogenous *Fgf21* (Fisher & Maratos-Flier, 2016). It is a possibility that the A^Y mice are experiencing an *Fgf21* resistant state and A^Y:Cpt1b$^{m-/-}$ mice remain sensitive to *Fgf21* via inhibition of skeletal muscle FAO, allowing for improved glucose utilization. However, this suggestion needs further investigation.

4.4. Investigation of Decreased Liver Weight in A^Y:Cpt1b$^{m-/-}$ Mice

Liver weights for A^Y:Cpt1b$^{m-/-}$ mice were significantly less than A^Y liver weights. Triglyceride and glycogen content were numerically lower in A^Y:Cpt1b$^{m-/-}$ mice and fluid levels were significantly less than A^Y mice. The correlation plot between fluid and glycogen + triglyceride content showed an R^2 value of 0.5. Increased amounts of triglycerides and glycogen content in the liver may be partially contributing to the increased fluid levels seen in the livers of A^Y mice. Increased fluid retention in the liver may also be suggestive of hepatic inflammation. Checking inflammatory biomarkers in the liver could potentially help with explaining the higher fluid levels seen in the A^Y mice.

Also, gene expression of various enzymes involved in fatty acid synthesis was upregulated in the livers of A^Y mice. Histology images show a larger amount of lipid

accumulation in A^Y liver relative to A^Y:Cpt1b$^{m-/-}$ liver. Taken together, these data suggest improvements in ectopic lipid accumulation in A^Y:Cpt1b$^{m-/-}$ liver relative to A^Y liver. These data also indicate that the addition of the Cpt1b$^{m-/-}$ to the A^Y heterozygote genotype results in a moderate, but important improvement in handling dietary energy.

4.5. Lower Respiratory Quotient in A^Y:Cpt1b$^{m-/-}$ Mice Relative to A^Y Mice

Pck1 was significantly elevated in the livers of A^Y:Cpt1b$^{m-/-}$ mice suggesting an upregulation in hepatic gluconeogenesis. Coupled with numerically lower liver glycogen, the increased amounts of liver *Pck1* and decreased FAO indicate that the glucose product of gluconeogenesis is being used for energy in the A^Y:Cpt1b$^{m-/-}$ mice. Despite these findings, the respiratory quotient for A^Y:Cpt1b$^{m-/-}$ mice was less than that of A^Y mice. This would suggest that the A^Y:Cpt1b$^{m-/-}$ mice were actually utilizing more fat for fuel relative to A^Y mice. Since the A^Y mice are hyperglycemic, they may have a higher RQ because glucose is more readily available for use. Additionally, enzymes involved with amino acid oxidation were upregulated in the skeletal muscle of A^Y:Cpt1b$^{m-/-}$ mice, suggesting an increase in the reliance on protein as a fuel source. Protein may be contributing to the decreased RQ seen in the A^Y:Cpt1b$^{m-/-}$ mice; however, it is likely to be minimal.

4.6. Possible Impact of *Gdf15*

Circulating triglycerides in serum of A^Y:Cpt1b$^{m-/-}$ mice fasted for 4 hours was found to be significantly less relative to A^Y mice. While hepatic triglycerides content in A^Y:Cpt1b$^{m-/-}$ mice were numerically lower than for A^Y mice, triglyceride content in circulation was significantly lower in A^Y:Cpt1b$^{m-/-}$ mice. Livers of A^Y:Cpt1b$^{m-/-}$ mice appear to be holding on to hepatic triglycerides rather than releasing into circulation, despite having numerically lower hepatic triglycerides. Interestingly, hepatic expression of *Gdf15* was found to be upregulated in A^Y liver compared to the other groups of mice. Previous research has found that *Gdf15* stimulated export of hepatic triglycerides into plasma serum (Luan et al., 2019). An increase in lipid levels in any specific tissue seems to correlate in the literature and in our models with an increase in the amount of *Gdf15* released from tissue (Lee et al., 2017; Li, Zhang, & Zhong, 2018). In our model, A^Y mice have large amounts of ectopic lipid in the liver along with elevated expression of hepatic *Gdf15* and elevated triglycerides in circulation. While not conclusive, lipid overload appears to lead to an induction of hepatic *Gdf15* and could potentially be indicative of pathology.

Gdf15 has also been found to help stimulate weight loss and improve glucose tolerance (Day et al., 2019). *Gdf15* is known to behave similarly to *Fgf21* in that both are stress induced hormones. Notably, *Gdf15* and *Fgf21* were found to follow the same pattern in gastrocnemius of all four mouse models included in this study. Given that *Fgf21* has an established role in the improvement of metabolic health in Cpt1b$^{m-/-}$ mice (Vandanmagsar et al., 2016), this raises the question of whether or not similar results would be found in a double knock out mouse model of *Cpt1b* and *Gdf15*. If *Gdf15* was found to have a similar affect as *Fgf21* on Cpt1b$^{m-/-}$ mice, this would raise the question of why do different physiological conditions lead to the release of these hormones from different sources and what does the source suggest? Hepatic release of *Gdf15* could possibly be suggestive of pathology while skeletal muscle release might indicate a favorable adaptation.

4.7. Limitations and Suggestions for Future Work

A large limitation to this pilot study is a low number of mice. Further investigation is needed with a larger number of mice per group. In future studies, the measurement of the phosphorylation of the α-subunit of AMPK at Thr-172 in A^Y:Cpt1b$^{m-/-}$ mice relative to Control and A^Y mice would further elaborate the metabolic effects of the skeletal muscle homozygote knock out of *Cpt1b*. Chemical analysis of triglycerides in the liver, serum and histology images of ectopic fat in the liver were the only lipid measure that we assessed. There are other lipids that we have not quantified but the triglyceride content provides evidence that fats were decreased in serum and liver. It would be worthwhile to have the hepatic histology images scanned in order to quantify the amount of lipid droplets shown in these images. We recommend that future studies should also quantify other fats in the liver and serum. Creation of a double knockout mouse model of skeletal muscle specific Cpt1b$^{m-/-}$ and *Gdf15* is recommended to determine if *Gdf15* plays a favorable role in the improved glucose utilization in Cpt1b$^{m-/-}$ mice. In addition to this, creation of a liver specific *Gdf15* knockout in A^Y mice is also recommended to determine if hepatic *Gdf15* influences plasma triglyceride levels. Further investigation is needed to determine additional factors contributing to the improved metabolic health when *Cpt1b* is knocked out in skeletal muscle. Transcriptomics and proteomic analyses of A^Y and A^Y:Cpt1b$^{m-/-}$ mice would be worthwhile in order to determine potential transcriptomes and proteomes contributing to the ameliorated glucose utilization and insulin sensitivity.

Previous transcriptomic analysis of Cpt1b$^{m-/-}$ mice showed that *Gdf15* was upregulated relative to control mice. Cpt1b$^{m-/-}$ mice had significantly less fat mass and body weight relative to control mice. The reasons for this leaner phenotype are not fully understood; however, increases in *Gdf15* may contribute to the decreases in fat mass and body weight. Gene expression showed that A^Y:Cpt1b$^{m-/-}$ mice also have increased expression of *Gdf15* in skeletal muscle relative to A^Y mice. Given that *Gdf15* is an anorectic hormone, one might expect this increase in expression to lead to weight loss in A^Y:Cpt1b$^{m-/-}$ mice relative to A^Y mice. However, differences in weight and fat mass were minimal and not significantly different between groups. This lack of weight loss might suggest that the ubiquitous expression of agouti is interfering with the signaling of *Gdf15* with receptors in the brain. *Gdf15* is known to bind to the Gfral receptor in the brain. We think *Gdf15* may also signal additional receptors in the brain.

We know the ubiquitous overexpression of agouti blocks the Mcr4, preventing alpha-melanocyte stimulating hormone from binding and driving yellow obese syndrome in A^Y mice. We suspected that this blockage of Mcr4 by agouti could also be interfering with the signaling of *Gdf15,* thus preventing the anorectic implications of this hormone. However, *Gdf15* has been found to reverse hyperphagia and obesity in a melanocortin 4 receptor deficient rat model (Hsu et al., 2017). Therefore, *Gdf15* does not appear to signal the Mcr4 receptor. It is still possible that *Gdf15* could signal other receptors in the brain besides Gfral and additional research is needed to determine this. If *Gdf15* is found to be responsible for the leaner phenotype in the Cpt1b$^{m-/-}$ mice, then the lack of weight loss seen in the A^Y:Cpt1b$^{m-/-}$ mice may suggest that the overexpression of agouti is also somehow interfering with the signaling of *Gdf15* in the A^Y:Cpt1b$^{m-/-}$ mice. *Gdf15* will need to be knocked out in Cpt1b$^{m-/-}$ mice to determine if it is responsible for any of the improvements in metabolic health seen in the Cpt1b$^{m-/-}$ mice. Additionally, if knocking out *Gdf15* in Cpt1b$^{m-/-}$ mice results in diminished weight loss, then the next step would be to knock out Gfral in Cpt1b$^{m-/-}$ mice in order to determine if other receptors are involved in the signaling

of *Gdf15.* If knocking out Mcr4 in the brain of Cpt1b$^{m-/-}$ mice still resulted in a leaner phenotype, then this would be one way to further confirm that *Gdf15* does not signal the Mcr4 receptor. The further investigation of the leaner phenotype found in Cpt1b$^{m-/-}$ mice could potentially help with furthering the understanding of *Gdf15* signaling in the brain.

4.8. Applications to the Treatment of Obesity and Diabetes

Inhibition of long chain fatty acid B-oxidation has proven to be effective for improving insulin sensitivity and glucose utilization in two mouse models, including one model of genetic obesity. In fact, inhibition of skeletal muscle long chain fatty acid B-oxidation resulted in a leaner phenotype in regular C57BL/6 mice. Genetically obese A^Y mice managed to maintain their obesity despite inhibition of long chain fatty acid B-oxidation in skeletal muscle. Further investigation is needed to fully understand what causes and protects against a leaner phenotype in each of these models, respectively. As of now, inhibition of *Cpt1b* in skeletal muscle appears to offer a therapeutic target for the treatment of insulin resistance. Currently, the three known inhibitors of *Cpt1* are Etomoxir, Oxfenicine and Perhexiline CPT-I. Unfortunately, it is hard for these inhibitors to specifically target skeletal muscle without negatively impacting the heart and liver as well. The potential for *Cpt1b* to serve as a pharmacological therapy for skeletal muscle insulin resistance is limited until the specificity of these inhibitors is established. Additional research will be needed in order to make this into an efficacious treatment plan.

4.9. Concluding Thoughts

In aggregate, our results showed *Cpt1b* inhibition in skeletal muscle to be efficacious from a treatment standpoint for improving insulin resistance even in the Agouti mouse model with severe obesity and diabetes, despite no significant change in adiposity. Overall, inhibition of long chain fatty acid B-oxidation in skeletal muscle of A^Y mice has proven to embody a mouse model in a metabolically healthy, yet obese state. Further investigation is needed in order to unveil the mechanisms driving the improvements in metabolic health that are observed when *Cpt1b* is inhibited in skeletal muscle.

Works Cited

Badin, P. M., Louche, K., Mairal, A., Liebisch, G., Schmitz, G., Rustan, A. C., . . . Moro, C. (2011). Altered skeletal muscle lipase expression and activity contribute to insulin resistance in humans. *Diabetes, 60*(6), 1734-1742. doi:10.2337/db10-1364

Bruce, C. R., Hoy, A. J., Turner, N., Watt, M. J., Allen, T. L., Carpenter, K., . . . Kraegen, E. W. (2009). Overexpression of carnitine palmitoyltransferase-1 in skeletal muscle is sufficient to enhance fatty acid oxidation and improve high-fat diet-induced insulin resistance. *Diabetes, 58*(3), 550-558. doi:10.2337/db08-1078

Cobb, J., & Dukes, I. (1998). Chapter 21 - Recent Advances in the Development of Agents for the Treatment of Type 2 Diabetes. In J. A. Bristol (Ed.), *Annual Reports in Medicinal Chemistry* (Vol. 33, pp. 213-222): Academic Press.

Day, E. A., Ford, R. J., Smith, B. K., Mohammadi-Shemirani, P., Morrow, M. R., Gutgesell, R. M., . . . Steinberg, G. R. (2019). Metformin-induced increases in GDF15 are important for suppressing appetite and promoting weight loss. *Nature Metabolism, 1*(12), 1202-1208. doi:10.1038/s42255-019-0146-4

Dutia, R., Kim, A. J., Modes, M., Rothlein, R., Shen, J. M., Tian, Y. E., . . . Wardlaw, S. L. (2013). Effects of AgRP inhibition on energy balance and metabolism in rodent models. *PloS one, 8*(6), e65317-e65317. doi:10.1371/journal.pone.0065317

Finck, B. N., Bernal-Mizrachi, C., Han, D. H., Coleman, T., Sambandam, N., LaRiviere, L. L., . . . Kelly, D. P. (2005). A potential link between muscle peroxisome proliferator- activated receptor-alpha signaling and obesity-related diabetes. *Cell Metab, 1*(2), 133-144. doi:10.1016/j.cmet.2005.01.006

Fisher, F. M., & Maratos-Flier, E. (2016). Understanding the Physiology of FGF21. *Annu Rev Physiol, 78*, 223-241. doi:10.1146/annurev-physiol-021115-105339

Hardy, O. T., Czech, M. P., & Corvera, S. (2012). What causes the insulin resistance underlying obesity? *Curr Opin Endocrinol Diabetes Obes, 19*(2), 81-87. doi:10.1097/MED.0b013e3283514e13

Hsu, J. Y., Crawley, S., Chen, M., Ayupova, D. A., Lindhout, D. A., Higbee, J., . . . Allan, B. B. (2017). Non-homeostatic body weight regulation through a brainstem-restricted receptor for GDF15. *Nature, 550*(7675), 255-259. doi:10.1038/nature24042

Iwatsuka, H., Shino, A., & Suzuoki, Z. (1970). General Survey of Diabetic Features of Yellow KK Mice. *Endocrinologia Japonica, 17*(1), 23-35. doi:10.1507/endocrj1954.17.23

Kelly, R., Alonso, S., Tajbakhsh, S., Cossu, G., & Buckingham, M. (1995). Myosin Light Chain 3F Regulatory Sequences Confer Regionalized Cardiac and Skeletal Muscle Expression in Transgenic Mice. *The Journal of Cell Biology, 129*(2), 383-396.

Keung, W., Ussher, J. R., Jaswal, J. S., Raubenheimer, M., Lam, V. H., Wagg, C. S., & Lopaschuk, G. D. (2013). Inhibition of carnitine palmitoyltransferase-1 activity alleviates insulin resistance in diet-induced obese mice. *Diabetes, 62*(3), 711-720. doi:10.2337/db12-0259

Kim, T., He, L., Johnson, M. S., Li, Y., Zeng, L., Ding, Y., . . . Yang, Q. (2014). Carnitine Palmitoyltransferase 1b Deficiency Protects Mice from Diet-Induced Insulin Resistance. *J Diabetes Metab, 5*(4), 361. doi:10.4172/2155-6156.1000361

Kim, T., Moore, J. F., Sharer, J. D., Yang, K., Wood, P. A., & Yang, Q. (2014). Carnitine Palmitoyltransferase 1b Deficient Mice Develop Severe Insulin Resistance After Prolonged High Fat Diet Feeding. *J Diabetes Metab, 5*. doi:10.4172/2155-6156.1000401

Knowler, W. C. B.-C., E.; Fowler, S. E.; Hamman, R. F.; Lachin, J. M.; Walker, E. A.; Nathan, D. M. (2002). Reduction in the incidence of type 2 diabetes with lifestyle intervention or metformin. *New England Journal of Medicine, 346*(6), 393-403.

Koegler, F. H., Schafffhauser, A. O., Mynatt, R. L., York, D. A., & Bary, G. A. (1999). Macronutrient Diet Intake of the Lethal Yellow Agouti (A y/a) Mouse. *Physiology & Behavior, 67*, 809-812.

Koves, T. R., Ussher, J. R., Noland, R. C., Slentz, D., Mosedale, M., Ilkayeva, O., . . . Muoio, D. M. (2008). Mitochondrial overload and incomplete fatty acid oxidation contribute to skeletal muscle insulin resistance. *Cell Metab, 7*(1), 45-56. doi:10.1016/j.cmet.2007.10.013

Laboratory, J. (2006). The Cre-lox and FLP-FRT systems. *JAX NOTES*.

Lee, J., Choi, J., Selen Alpergin, E. S., Zhao, L., Hartung, T., Scafidi, S., . . . Wolfgang, M. J. (2017). Loss of Hepatic Mitochondrial Long-Chain Fatty Acid Oxidation Confers Resistance to Diet-Induced Obesity and Glucose Intolerance. *Cell Rep, 20*(3), 655-667. doi:10.1016/j.celrep.2017.06.080

Li, D., Zhang, H., & Zhong, Y. (2018). Hepatic GDF15 is regulated by CHOP of the unfolded protein response and alleviates NAFLD progression in obese mice. *Biochem Biophys Res Commun, 498*(3), 388-394. doi:10.1016/j.bbrc.2017.08.096

Luan, H. H., Wang, A., Hilliard, B. K., Carvalho, F., Rosen, C. E., Ahasic, A. M., . . . Medzhitov, R. (2019). GDF15 Is an Inflammation-Induced Central Mediator of Tissue Tolerance. *Cell, 178*(5), 1231-1244 e1211. doi:10.1016/j.cell.2019.07.033

Michaud, E. J., Bultman, S. J., Klebig, M. L., van Vugt, M. J., Stubbs, L. J., Russell, L. B., & Woychik, R. P. (1994). A molecular model for the genetic and phenotypic characteristics of the mouse lethal yellow (Ay) mutation. *Proceedings of the National Academy of Sciences, 91*(7), 2562-2566. doi:10.1073/pnas.91.7.2562

Miltenberger, R. J., Mynatt, R. L., Wilkinson, J. E., & Woychik, R. P. (1997). The Role of the agouti Gene in the Yellow Obese Syndrome. *The Journal of Nutrition, 127*(9), 1902S-1907S. doi:10.1093/jn/127.9.1902S

Nachman, M. W., Hoekstra, H. E., & D'Agostino, S. L. (2003). The genetic basis of adaptive melanism in pocket mice. *Proceedings of the National Academy of Sciences, 100*(9), 5268-5273. doi:10.1073/pnas.0431157100

O'Neill, H. M. (2013). AMPK and Exercise: Glucose Uptake and Insulin Sensitivity. *Diabetes Metab J, 37*(1), 1-21. doi:10.4093/dmj.2013.37.1.1

Ollmann, M. M., Lamoreux, M. L., Wilson, B. D., & Barsh, G. S. . (1998). Interaction of Agouti protein with the melanocortin 1 receptor in vitro and in vivo. *Genes & development, 12*(3), 316-330.

Pagel-Langenickel, I., Bao, J., Pang, L., & Sack, M. N. (2010). The role of mitochondria in the pathophysiology of skeletal muscle insulin resistance. *Endocr Rev, 31*(1), 25-51. doi:10.1210/er.2009-0003

Perdomo, G., Commerford, S. R., Richard, A. M., Adams, S. H., Corkey, B. E., O'Doherty, R. M., & Brown, N. F. (2004). Increased beta-oxidation in muscle cells enhances insulin-stimulated glucose metabolism and protects against fatty acid-induced insulin resistance despite intramyocellular lipid accumulation. *J Biol Chem, 279*(26), 27177-27186. doi:10.1074/jbc.M403566200

Rufer, A. C., Thoma, R., & Hennig, M. (2009). Structural insight into function and regulation of carnitine palmitoyltransferase. *Cellular and Molecular Life Sciences, 66*(15), 2489-2501. doi:10.1007/s00018-009-0035-1

Sebastian, D., Herrero, L., Serra, D., Asins, G., & Hegardt, F. G. (2007). CPT I overexpression protects L6E9 muscle cells from fatty acid-induced insulin resistance. *Am J Physiol Endocrinol Metab, 292*(3), E677-686. doi:10.1152/ajpendo.00360.2006

Tao, Y.-X. (2010). The melanocortin-4 receptor: physiology, pharmacology, and pathophysiology. *Endocrine reviews, 31*(4), 506-543. doi:10.1210/er.2009-0037

Vandanmagsar, B., Warfel, J. D., Wicks, S. E., Ghosh, S., Salbaum, J. M., Burk, D., . . . Mynatt, R. L. (2016). Impaired Mitochondrial Fat Oxidation Induces FGF21 in Muscle. *Cell Rep, 15*(8), 1686-1699. doi:10.1016/j.celrep.2016.04.057

Wang, O., & Majzoub, J. A. (2011). Chapter 3 - Adrenocorticotropin. In S. Melmed (Ed.), *The Pituitary (Third Edition)* (pp. 47-81). San Diego: Academic Press.

Warfel, J. D., Bermudez, E. M., Mendoza, T. M., Ghosh, S., Zhang, J., Elks, C. M., . . . Vandanmagsar, B. (2016). Mitochondrial fat oxidation is essential for lipid-induced inflammation in skeletal muscle in mice. *Sci Rep, 6*, 37941. doi:10.1038/srep37941

Warfel, J. D., Vandanmagsar, B., Wicks, S. E., Zhang, J., Noland, R. C., & Mynatt, R. L. (2017). A low fat diet ameliorates pathology but retains beneficial effects associated with CPT1b knockout in skeletal muscle. *PloS one, 12*(12), e0188850. doi:10.1371/journal.pone.0188850

Wicks, S. E., Vandanmagsar, B., Haynie, K. R., Fuller, S. E., Warfel, J. D., Stephens, J. M., . . . Mynatt, R. L. (2015). Impaired mitochondrial fat oxidation induces adaptive remodeling of muscle metabolism. *Proc Natl Acad Sci U S A, 112*(25), E3300-3309. doi:10.1073/pnas.1418560112

Wicks, S. E., Vandanmagsar, B., Haynie, K. R., Fuller, S. E., Warfel, J. D., Stephens, J. M., . . . Mynatt, R. L. (2015). Impaired mitochondrial fat oxidation induces adaptive remodeling of muscle metabolism. *Proceedings of the National Academy of Sciences, 112*(25), E3300-E3309. doi:10.1073/pnas.1418560112

Wilson-Fritch, L., Nicoloro, S., Chouinard, M., Lazar, M. A., Chui, P. C., Leszyk, J., . . . Corvera, S. (2004). Mitochondrial remodeling in adipose tissue associated with obesity and treatment with rosiglitazone. *J Clin Invest, 114*(9), 1281-1289. doi:10.1172/JCI21752

Vita

Allison Stone, received her bachelor's degree from Southeastern Louisiana University in 2017. She decided to go back to school to pursue a master's degree in 2018. As her interest in health and wellness grew, she decided to enter the Department of Nutrition and Food Sciences at Louisiana State University. Upon completion of her master's degree, she plans to continue to expand her knowledge in the field of health and wellness.